The Plant Cell, Vol. 26: 373–390, January 2014, www.plantcell.org

Thylakoid FtsH Protease Contributes to Photosystem II and Cytochrome b_6f Remodeling in *Chlamydomonas reinhardtii* under Stress Conditions[W]

Alizée Malnoë,[1] Fei Wang, Jacqueline Girard-Bascou, Francis-André Wollman, and Catherine de Vitry[2]

Institut de Biologie Physico-Chimique, Unité Mixte de Recherche 7141, Centre National de la Recherche Scientifique/Université Pierre et Marie Curie, Paris 6, 75005 Paris, France

FtsH is the major thylakoid membrane protease found in organisms performing oxygenic photosynthesis. Here, we show that FtsH from *Chlamydomonas reinhardtii* forms heterooligomers comprising two subunits, FtsH1 and FtsH2. We characterized this protease using FtsH mutants that we identified through a genetic suppressor approach that restored phototrophic growth of mutants originally defective for cytochrome b_6f accumulation. We thus extended the spectrum of FtsH substrates in the thylakoid membranes beyond photosystem II, showing the susceptibility of cytochrome b_6f complexes (and proteins involved in the c_i heme binding pathway to cytochrome b_6) to FtsH. We then show how FtsH is involved in the response of *C. reinhardtii* to macronutrient stress. Upon phosphorus starvation, photosynthesis inactivation results from an FtsH-sensitive photoinhibition process. In contrast, we identified an FtsH-dependent loss of photosystem II and cytochrome b_6f complexes in darkness upon sulfur deprivation. The D1 fragmentation pattern observed in the latter condition was similar to that observed in photoinhibitory conditions, which points to a similar degradation pathway in these two widely different environmental conditions. Our experiments thus provide extensive evidence that FtsH plays a major role in the quality control of thylakoid membrane proteins and in the response of *C. reinhardtii* to light and macronutrient stress.

INTRODUCTION

Photosynthesis allows the conversion of light energy, captured by chlorophyll–protein complexes, into reducing power (NADPH) and chemical energy (ATP). In oxygenic photosynthesis, the photoinduced reduction of $NADP^+$ is performed by a photosynthetic electron transfer chain, which joins three major oligomeric proteins embedded in the thylakoid membranes: photosystem II (PSII), cytochrome b_6f complex, and photosystem I (PSI). The assembly, degradation and repair of these protein complexes require some coordination in the expression of numerous subunits encoded either in the chloroplast or in the nucleus, to which numerous cofactors such as chlorophylls, carotenoids, hemes, and iron-sulfur clusters must be added. The traffic of these proteins and of their molecular cofactors to their proper destination requires the action of a diverse set of chaperones, assembly factors, and proteases that ensure the proper biogenesis and recycling of these heterooligomeric complexes.

In recent years, the field of chloroplast protease studies has drawn increasing interest because of their role in the response to oxidative stress that results from the reaction of molecular oxygen with radical species, both of which are produced during illumination of the photosynthetic apparatus. Genomic and proteomic studies provided extensive identification of a well-defined set of chloroplast proteases of bacterial origin (reviewed in Sokolenko et al., 2002; Adam et al., 2006; Sakamoto, 2006; Huesgen et al., 2009), most of which are encoded by nuclear genes, with the exception of the catalytic subunit ClpP1 of the Clp protease, which is chloroplast encoded. Together with Clp, the Deg and FtsH proteases are the major proteolytic enzymes whose activities have been implicated in the regulation of biogenesis and the repair of photosynthetic proteins. A variety of studies proposed a role of these proteases in PSII repair upon photoinhibition (Lindahl et al., 2000; Majeran et al., 2001; Bailey et al., 2002; Silva et al., 2003; Kapri-Pardes et al., 2007; Kato and Sakamoto, 2009; Kato et al., 2012). However, we still have limited knowledge of the diversity of their substrates and regulatory functions.

The thylakoid membrane–anchored ATP-dependent protease FtsH is involved in the processive degradation of stroma-exposed thylakoid proteins, both in *Arabidopsis thaliana* and the cyanobacterium *Synechocystis* (reviewed in Lindahl et al., 1996; Narberhaus et al., 2009; Rodrigues et al., 2011). FtsH is a member of the large and diverse AAA+ (for ATPase associated with diverse cellular activities) protein family (Neuwald et al., 1999). It contains an ATPase domain with Walker A and B motifs and a second region of homology (SRH) with a protease domain displaying a zinc binding motif. FtsH is the only membrane-anchored and essential ATP-dependent protease in *Escherichia coli*, and it participates in protein quality control for only a few known membrane-bound and cytoplasmic substrates (Suzuki et al., 1997; Herman et al., 2003; Ito and Akiyama, 2005; Narberhaus et al., 2009). It has been suggested based on study in *E. coli* that ATPase activity is required for pulling out substrate proteins from the membrane and pushing them into the internal pore of the FtsH ring structure for proteolysis (Ito and Akiyama, 2005). While FtsH is encoded by a unique gene in most prokaryotes, multiple isoforms are found in plants, algae, and cyanobacteria (see the phylogenetic tree of FtsH homologs in

[1] Current address: Department of Plant and Microbial Biology, University of California, Berkeley, CA 94720-3102.
[2] Address correspondence to catherine.devitry@ibpc.fr.
The author responsible for distribution of materials integral to the findings presented in this article in accordance with the policy described in the Instructions for Authors (www.plantcell.org) is: Catherine de Vitry (catherine.devitry@ibpc.fr).
[W] Online version contains Web-only data.
www.plantcell.org/cgi/doi/10.1105/tpc.113.120113

Supplemental Figure 1). Characterization of the functional contribution of these isoforms has only started and combines in vivo and in vitro approaches. Four FtsH homologs (FtsH1 to FtsH4) are found in *Synechocystis* sp PCC 6803: FtsH3 copurifies with FtsH2 or FtsH1 in heterohexamers (Boehm et al., 2012). In *Arabidopsis*, the 12 nucleus-encoded FtsH family members (FtsH1 to FtsH12) are distributed between mitochondria and chloroplasts; in addition, five *Arabidopsis* FtsH-like proteins (FtsHi1 to FtsHi5) targeted to the chloroplast envelope lack the conserved zinc binding motif HisGluXxxXxxHis and are presumably inactive as protease (reviewed in Wagner et al., 2012; see also *Arabidopsis* proteome databases [Sun et al., 2009; Ferro et al., 2010]). Four isoforms have been identified in *Arabidopsis* thylakoid membranes: two of type A (FtsH1 and FtsH5) and two of type B (FtsH2 and FtsH8; Friso et al., 2004). The thylakoid enzyme is made of an active heterohexameric ring structure containing type A and B subunits whose accumulation is concerted, with a proposed stoichiometry of two type A and four type B subunits (Zaltsman et al., 2005; Moldavski et al., 2012) or three type A and three type B subunits (Yu et al., 2004; Boehm et al., 2012). *Arabidopsis* type A and type B subunits use different membrane insertion pathways (Rodrigues et al., 2011).

Here, we isolated two mutants in the gene encoding the thylakoid-embedded FtsH1 protein in the unicellular green alga *Chlamydomonas reinhardtii*. These mutants were recovered in a genetic screen to identify proteases that would target cytochrome b_6f complex to degradation. The cytochrome b_6f complex differs from bc_1 by an additional c_i heme located at the quinone reduction site (Kurisu et al., 2003; Stroebel et al., 2003). In recent years, we characterized cofactor assembly to complex C subunit B (CCB) factors involved in the covalent binding of c_i heme to Cys-35 of cytochrome b_6 in *C. reinhardtii* (Kuras et al., 1997, 2007) and *Arabidopsis* (Lezhneva et al., 2008). Mutants lacking c_i heme cannot grow photoautotrophically because they show too little accumulation of a dysfunctional b_6f complex (Saint-Marcoux et al., 2009). This observation provided the basis of a screen for suppressor mutations that affected FtsH and restored higher accumulation of dysfunctional b_6f complexes to a level sufficient to sustain phototrophic growth.

Here, we show that the thylakoid-bound FtsH protease from *C. reinhardtii* is mainly found in heterooligomers, larger than 1 MD, comprising two subunits: FtsH1 and FtsH2. Mutation of an Arg residue required for ATP hydrolysis in FtsH1 hampers the integration of the whole FtsH protease in these large supercomplexes and impairs the processive degradation of photosynthetic membrane proteins, especially when they are difficult to unfold. In particular, we investigate the role of FtsH in PSII repair upon *C. reinhardtii* photoinhibition, described by others in cyanobacteria and plant chloroplasts, but we extend its function to the regulation of PSII accumulation upon macronutrient stress as well as to the quality control of neosynthesized cytochrome b_6f complexes.

RESULTS

A Genetic Suppressor Approach to Obtaining Protease Mutants in *C. reinhardtii*

In a previous study (de Vitry et al., 2004), we had shown that *ccb* mutants of *C. reinhardtii*, which are nonphototrophic as a result of their inability to bind c_i heme to apocytochrome b_6, accumulate very low amounts of b_6f complex subunits. However, Blue Native (BN)-PAGE showed that these remaining subunits still assembled into oligomeric complexes corresponding to cytochrome b_6f dimers, similar to those found in the wild-type strain. In addition, we gathered preliminary evidence that these b_6f complexes retained some electron transfer properties, as detected by their fluorescence induction kinetics, which pointed to some reoxidation of the plastoquinol pool under continuous illumination (Saint-Marcoux et al., 2009).

In a search for phototrophic suppressors, we performed a UV light mutagenesis of nuclear *ccb* mutants and selected revertants for their ability to grow on minimal medium (Figure 1A). Some of these, as illustrated by strain *Rccb2-303* (Figure 1B), showed wild-type levels of b_6f complexes together with a restoration of heme c_i binding, as viewed by the recovery of a heme-stained cytochrome b_6 upon electrophoresis, whereas others, as exemplified by *Rccb2-306* and *Rccb4-301* in Figure 1B, still lacked c_i heme, despite a wild-type accumulation of cytochrome b_6f subunits. The latter strains were promising candidates for being protease mutants unable to degrade b_6f complexes lacking heme c_i. In further support of this hypothesis, Figure 1B shows that *Rccb2-306* also recovered wild-type levels of CCB4, which was hardly detectable in the original *ccb2* mutant, owing to its concerted accumulation with CCB2 (Saint-Marcoux et al., 2009), and reciprocally, *Rccb4-301* recovered some CCB2. We note that CCB2 is detected as a doublet in the absence of CCB4, as we observed previously (Saint-Marcoux et al., 2009).

In a backcross between *Rccb2-306* and the original *ccb2* mutant, we observed only parental ditype tetrads with a Mendelian segregation of cytochrome b_6f accumulation and phototrophy, which indicated that the revertant phenotype was due to a single suppressor mutation in the nuclear genome (Supplemental Figure 2). The cross between revertant *Rccb2-306* and the wild-type strain yielded 2 parental ditype and 10 tetratype tetrads, indicative of an extragenic suppressor mutation, unlinked to the *CCB2* gene. We isolated solely the suppressor named $Su_{1\text{-}ccb2}$ from a tetratype tetrad and characterized its phenotype (Figure 2). The suppressor effect of $Su_{1\text{-}ccb2}$ was confirmed by crossing it back to *ccb2* (Supplemental Figure 3). Figure 2A shows that the contents of cytochrome b_6f subunits and of CCB2/4 proteins in the suppressor $Su_{1\text{-}ccb2}$ were undistinguishable from those in the wild-type strain. The photosynthetic electron transfer properties were examined in vivo on dark-adapted cells by fluorescence induction kinetics under continuous illumination, giving initial and steady state fluorescence in the light, followed by a saturating pulse to determine maximal fluorescence (F_m). These values allow calculation of the maximum quantum efficiency of PSII primary photochemistry, (F_m − initial fluorescence in the light)/F_m, denoted F_v/F_m, and the quantum yield of PSII photochemistry, (F_m − steady state fluorescence in the light)/F_m, denoted ΦPSII (Genty et al., 1989; Baker, 2008). The *ccb2* mutant could be identified by its fluorescence yield, which rose continuously to a stationary fluorescence level close to F_m. The double mutant *Rccb2* displayed fluorescence kinetics and ΦPSII intermediate between those in *ccb2* and wild-type strains. When $Su_{1\text{-}ccb2}$ was grown under low light, F_v/F_m and ΦPSII were decreased yet comparable to the wild-type strain, indicative of an

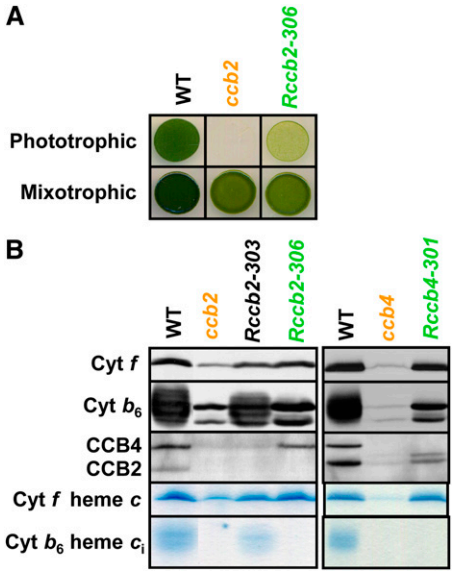

Figure 1. Revertants Recovered the Wild-Type Level of b_6f Complexes.

(A) Phototrophic growth on minimal medium and mixotrophic growth control on acetate medium at 10 μE m^{-2} s^{-1}.
(B) Total cell proteins of the wild type, *ccb2* and *ccb4* mutants, and *Rccb2-303*, *Rccb2-306*, and *Rccb4-301* revertants grown in acetate medium at 6 μE m^{-2} s^{-1} were separated by SDS/urea-PAGE and analyzed by immunodetection with antibodies against cytochrome b_6f subunits (cytochrome *f* and cytochrome b_6) and CCB factors involved in the covalent binding of c_i heme to cytochrome b_6 (CCB2 and CCB4) and by heme peroxidase activity detection using tetramethylbenzamidine.

efficient photosynthetic electron transfer (Figure 2B). However, when grown at higher light intensity, the suppressor mutant $Su_{1\text{-}ccb2}$ underwent a considerable loss in F_v/F_m and ΦPSII, indicative of a nearly complete loss in PSII activity (Figure 2C). Its growth under high light was heavily compromised even under mixotrophic conditions (Figure 2D), an observation that led us to conclude that the suppressor mutation conferred a highly photosensitive phenotype to the $Su_{1\text{-}ccb2}$ strain, a feature that we used for map-based cloning and molecular identification of the suppressor mutation.

Map-Based Cloning of the Point Mutation *ftsh1-1*

The above $Su_{1\text{-}ccb2}$ phenotype did not offer a selection scheme for identification of the mutation by genetic complementation. Since it was obtained by UV light mutagenesis, it did not allow for the possibility to identify DNA-flanking regions as after insertional mutagenesis. As an alternative method, we used map-based cloning that relies on crosses of *C. reinhardtii* with the interfertile species *Chlamydomonas grossii* (also known as S1-D2 or CC-2290), which has a suitable profusion of genomic polymorphisms to permit the identification of the region bearing a mutation (Rymarquis et al., 2005). In each of 127 tetrads, we took one progeny carrying the $Su_{1\text{-}ccb2}$ mutation for linkage analysis to various markers. We localized the suppressor mutation on chromosome 12 in the vicinity of the PSR1 and BDF1 markers (Supplemental Figure 4). Next, we amplified and sequenced several candidate genes in this region and found a mutation in the gene encoding the protease FtsH1. The $Su_{1\text{-}ccb2}$ mutation is a CC-to-TT modification leading to a substitution of $Gly419_{GGC}Arg420_{CGC}$ into $Gly419_{GGT}Cys420_{TGC}$. In the following, the $Su_{1\text{-}ccb2}$ strain, which bears this *ftsH1-R420C* substitution, will be referred to as *ftsh1-1*. Similarly, the revertant *Rccb4-301* harbored an *ftsH1-T382I* mutation (*ftsh1-2*) with a $Thr382_{ACC}$ into $Ile382_{ATT}$ substitution. Both $Su_{1\text{-}ccb2}$ and *Rccb4-301* displayed a wild-type *FTSH2* sequence that encodes the other thylakoid-targeted subunit of the FtsH protease (see below). The mutated Arg and Thr residues are well conserved among FtsH sequences from various organisms and are located, respectively, in or before the SRH domain of the FtsH protein (Figures 3A and 3B). Several mutations of the conserved Arg-420 in *E. coli* were shown to compromise ATP hydrolysis and thereby the protease activity of FtsH homohexamers (Karata et al., 1999, 2001).

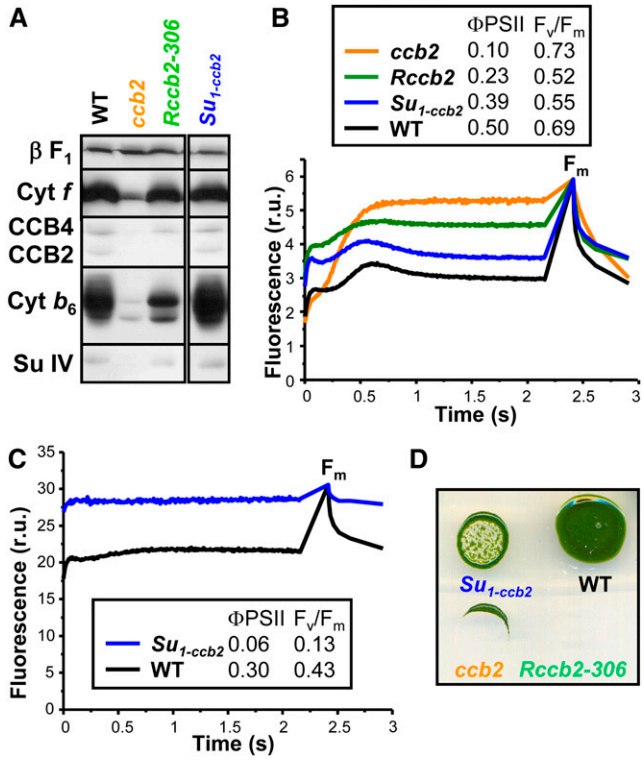

Figure 2. The Suppressor $Su_{1\text{-}ccb2}$ Is Photosensitive.

(A) Total proteins of cells grown at 6 μE m^{-2} s^{-1} separated by SDS/urea-PAGE and analyzed by immunodetection with antibodies against cytochrome b_6f subunits (cytochrome *f*, cytochrome b_6, and subunit IV) and CCB factors (CCB2 and CCB4), with the ATP synthase β-subunit (β F_1) as a loading control.
(B) Fluorescence induction kinetics in relative units (r.u.) at low actinic light of dark-adapted cells followed by a saturating pulse to determine F_m. Strains were grown at 6 μE m^{-2} s^{-1}.
(C) Fluorescence kinetics. Strains were grown at 6 μE m^{-2} s^{-1} followed by 16 h at 200 μE m^{-2} s^{-1}.
(D) Mixotrophic growth of the strains at 200 μE m^{-2} s^{-1}.

The *ftsh1-1* mutation is recessive, as demonstrated by the low accumulation of b_6f complex subunits observed in vegetative diploids from the cross *ftsh1-1 ccb2 arg7* × *FTSH1 ccb2 arg2* (Supplemental Figure 5). Transformation of the *ftsh1-1* and *ccb2 ftsh1-1* strains with the vector pSL18 containing *FTSH1* genomic DNA (pSL18-*FTSH1*) under the control of the *PSAD* promoter (see Methods) showed that *FTSH1* can complement the loss of PSII activity upon high-light treatment (Figures 4A and 4B) and restore a *ccb2* fluorescence phenotype (Figure 4C), respectively. Transformation of these strains with an empty vector (pSL18) did not change their fluorescence kinetics, demonstrating that the *FTSH1* gene alone was sufficient for complementation.

ftsh1-1 Still Allows Accumulation of the FtsH1-R420C Mutated Protein but Largely Impairs Its Oligomerization in High Molecular Mass Complexes

Thylakoid FtsH proteases form various heterohexamers in cyanobacteria (Boehm et al., 2012) and *Arabidopsis* (Sakamoto et al., 2003; Yu et al., 2004; Zaltsman et al., 2005; Moldavski et al., 2012). Whereas four isoforms of thylakoid FtsH were identified in *Arabidopsis* (Zaltsman et al., 2005), only two thylakoid isoforms, FtsH1 and FtsH2, have been identified by proteomic studies in *C. reinhardtii* (Allmer et al., 2006). We raised specific antibodies against peptides from each of these isoforms (see Methods). The immunoblots of Figure 3C show that neither the accumulation of FtsH1 nor that of FtsH2 was compromised in the *ftsh1-1* mutant. However, the mutated FtsH1-R420C protein migrates slightly higher than the wild-type FtsH1. We used these electrophoresis conditions, which separate the wild-type FtsH1 protein from the mutated one, to immunodetect their coexpression as a doublet in strains comprising the *ftsh1-1* mutation complemented with pSL18-*FTSH1* (Figure 4D).

To examine whether the *ftsh1-1* mutation altered the state of oligomerization of the thylakoid FtsH protease, we combined a mild digitonin solubilization of the thylakoid membranes with two-dimensional BN/SDS-PAGE to identify oligomeric forms of FtsH1 and FtsH2 in *C. reinhardtii* wild-type and *ftsh1-1* strains (Figure 3D). The two isoforms, FtsH1 and FtsH2, showed the same migration pattern, being mainly found in either of two populations, the smaller FtsH(S) and the larger FtsH(L) proteins. FtsH(L) is localized in the 1-MD region, as evidenced by its comigration with D1-containing PSII supercomplexes (Heinemeyer et al., 2004).

The presence of FtsH in PSII complexes was previously reported in cyanobacteria and *Arabidopsis* and proposed to allow immediate access to damaged D1 and thereby efficient D1 degradation (Kashino et al., 2002; Yoshioka et al., 2010). However, we could not coimmunoprecipitate PSII subunits with our antibody to FtsH1 (Supplemental Figure 6), which suggests either that these high molecular mass complexes merely comigrate in BN-PAGE or that they offer limited accessibility of the FtsH1 antigenic peptide.

FtsH(S) was found in the 150- to 200-kD region and is likely to correspond to an FtsH1/FtsH2 heterodimer. In stark contrast to the wild type, which displayed most of the FtsH1 and FtsH2 isoforms in the FtsH(L) population, up to approximately two-thirds of FtsH1 and FtsH2 were found in the FtsH(S) population in the *ftsh1-1* mutant. Notably, the PSII supercomplex level was decreased in the *ftsh1-1* mutant, in line with data on the *Arabidopsis* FtsH2 (*var2*) mutant (Kato et al., 2009). The similar distribution patterns of FtsH1 and FtsH2 suggested an interaction between the two within heterooligomers, which was confirmed by coimmunoprecipitation with purified antibodies against a peptide of FtsH1 that does not cross-react with FtsH2 (Figure 3E). In both the wild-type strain and the *ftsh1-1* mutant, FtsH2 was pulled down together with FtsH1. Therefore, the phenotype of the *ftsh1-1* mutant results from the expression of a defective enzyme that is still made of FtsH1/FtsH2 heterooligomers. However, the *ftsh1-1* mutation prevents the integration of most of the FtsH1/FtsH2 heterodimers in larger supercomplexes.

The Accumulation and Lifetime of Cytochrome b_6f Complexes Lacking c_i Heme Are Highly Increased in the *ftsh1-1* Context

The suppressor strategy that led us to the identification of the *ftsh1-1* mutant suggested that the assembled b_6f complex is a substrate for the FtsH protease. We combined, by genetic crosses, the *ftsh1-1* mutation with the {*petB-C35V*} mutation, which prevents covalent binding of heme c_i to cytochrome b_6 and leads to a low accumulation level of cytochrome b_6f complexes (de Vitry et al., 2004). As was the case for the *ccb2 ftsh1-1* mutant, the double mutant {*petB-C35V*} *ftsh1-1* now accumulated wild-type levels of b_6f complex subunits (compared with lanes 0 of the single and double mutants in Figure 5, right side). The accumulation of cytochrome b_6f subunits in mutants defective for c_i binding in the *ftsh1-1* mutated context is due to a decrease in their rate of degradation, as also shown in Figure 5. After blocking protein synthesis in the chloroplast with chloramphenicol at time 0, we observed (over the 8-h time span of the immunochase experiment) that the lifetime of cytochrome b_6 and subunit IV showed a considerable increase when the *ftsh1-1* mutation was introduced into strains containing a mutation that impedes the binding of c_i heme, as exemplified by the *ccb2* and {*petB-C35V*} mutations (Figures 5A and 5B). This result demonstrates that the higher accumulation of b_6f complexes in the double mutants is due to their lower rate of degradation. We attribute the limited degradation of b_6f complexes still occurring in the double mutants to some residual FtsH activity and/or to other proteases (see Discussion).

The *ftsh1-1* Mutation Increases PSII Sensitivity to Photoinhibition, Prevents PSII Repair, and Leads to the Accumulation of D1 Fragments

Photoinhibition, a common feature of light stress in plants, algae, and cyanobacteria, occurs when the rate of light-induced damage to PSII exceeds the repair capacity. The repair of PSII involves partial disassembly of the damaged complex, selective proteolytic degradation and replacement of the damaged subunit (predominantly the D1 reaction center subunit) by a de novo synthesized copy, and reassembly. In plants and cyanobacteria, FtsH regulates PSII repair, through its ability to digest photooxidatively damaged D1 proteins, either alone in cyanobacteria or in combination with Deg proteases in plants (reviewed in Kato

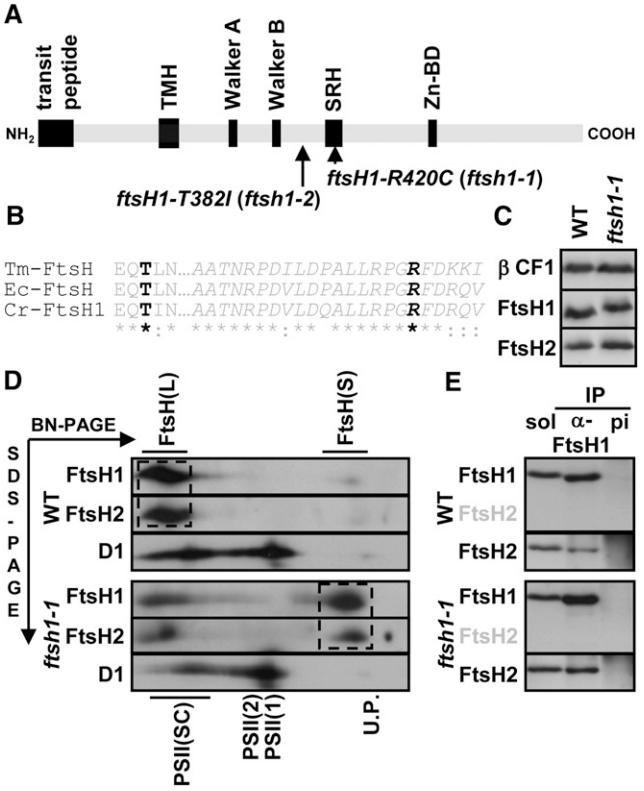

Figure 3. Mutant *ftsH1-R420C* Accumulates Wild-Type Levels of FtsH1 and FtsH2 but with Impaired Oligomerization.

(A) Schematic representation of ATP-dependent zinc metalloprotease FtsH1 with the transit peptide, one thylakoid transmembrane helix (TMH), ATPase Walker A and B motifs, the SRH containing conserved Arg residues required for ATP hydrolysis (one of which is substituted to a Cys residue in the *ftsH1-R420C* [*ftsh1-1*] mutant of *C. reinhardtii*), and the zinc binding domain (Zn-BD).

(B) Alignment of the SRH (in italics) from *T. maritima* FtsH (Tm-FtsH), *E. coli* FtsH (Ec-FtsH), and *C. reinhardtii* FtsH1 (Cr-FtsH1), indicating the conservation of the Arg and Thr residues (in black) substituted in the *ftsh1-1* and *ftsh1-2* mutants.

(C) Mutant *ftsH1-R420C* accumulates wild-type levels of FtsH1 and FtsH2. Total cell proteins were separated on an 8% polyacrylamide gel in the presence of 8 M urea and analyzed by immunodetection with specific antibodies against FtsH1, FtsH2, and the ATP synthase β-subunit (β CF1) as a loading control.

(D) FtsH complexes after BN-PAGE of digitonin-solubilized membranes from cells grown at 6 $\mu E\ m^{-2}\ s^{-1}$. Digitonin-solubilized proteins were separated in the first dimension by BN-PAGE (3 to 12%) and in the second dimension as in **(C)** and blotted onto a polyvinylidene difluoride membrane. The blot was sequentially probed with antibodies specific for FtsH2, FtsH1, and D1. FtsH1 and FtsH2 migrated mainly and similarly in two populations, the smaller FtsH(S) and the larger FtsH(L) proteins. FtsH (L) is abundant in the wild type and FtsH(S) in *ftsh1-1* (dashed boxes). The positions of unassembled proteins (U.P.), monomers [PSII(1)], dimers [PSII(2)], and supercomplexes [PSII(SC)] of PSII are indicated and used as molecular mass markers.

(E) Coimmunoprecipitation analysis of FtsH1 and FtsH2 interactions. Digitonin-solubilized membranes (prepared as for BN-PAGE) from the wild-type and *ftsh1-1* strains were incubated with protein A–Sepharose beads coupled to antibodies against a peptide of FtsH1 (α-FtsH1) or against preimmune serum (pi). Aliquots of digitonin-solubilized membranes (sol) and immunoprecipitates (IP) were separated as in **(C)** and analyzed by immunodetection with antibodies against FtsH1 (not cross-reacting with FtsH2, as indicated with gray letters) and FtsH2.

and Sakamoto, 2009; Nixon et al., 2010). The role of FtsH during algal photoinhibition is unclear, and the role of FtsH and the possible contribution of chloroplast Deg proteases to this process has not been confirmed experimentally. The *ftsh1-1* mutant enabled us to address these issues.

To explore further the strong decrease in F_v/F_m upon higher light exposure and the photosensitive growth phenotype of the *ftsh1-1* mutant observed in Figures 2C and 2D, we monitored PSII activity by measuring the F_v/F_m during a mild photoinhibition treatment (250 $\mu E\ m^{-2}\ s^{-1}$) and a subsequent recovery under low light (6 $\mu E\ m^{-2}\ s^{-1}$). The addition of inhibitors of chloroplast translation, lincomycin and chloramphenicol (LC), prevents D1 synthesis and permits the discrimination of photodamage from repair. As shown in Figure 6A, the *ftsh1-1* mutation dramatically increased PSII sensitivity to a mild photoinhibition: over a 1-h illumination period with photoinhibitory light, the loss in variable fluorescence was more extensive and developed faster (Figure 6A, inset) in the mutant than in the wild type, and most of the functional recovery was prevented in a subsequent low-light illumination period, irrespective of inhibitor addition. The means and SD of PSII activity recovery after 1.5 h were 63% ± 12% for the wild type and 19% ± 8% for the *ftsh1-1* mutant (three independent experiments). This lack of recovery is similar to what was observed in the wild-type strain when D1 synthesis was inhibited and thus delineates the important role of FtsH in the PSII repair cycle during algal photoinhibition.

Using antibodies against the DE loop or the C terminus of D1 (Figure 6B), we probed the fate of full-length D1 protein and the accumulation of D1 fragments in the same experiment, using longer exposure times of the immunoblots for proper detection of fragments (Figure 6C). Full-length D1 did not decrease during photoinhibition and recovery in the wild type or *ftsh1-1* unless translation inhibitors were added during the experiment (LC condition). In the latter condition, the loss of D1 was more extensive in the wild type than in the mutant, as viewed when probed with either of the two antibodies. However, D1 fragments accumulated mainly in the *ftsh1-1* mutant. They were detected around 23 kD with the anti-D1 DE loop (Figures 7B and 8B) and in the 16- to 20-kD and 6- to 10-kD regions with the anti-D1 C terminus. We note that the 6- to 10-kD D1 fragments were particularly abundant in *ftsh1-1* and even could be well detected before photoinhibitory treatment (Figure 6C). We quantified the content in D1 upon photoinhibition by chemiluminescence using the D1 C-terminal antibody and OEE2 as a loading control when repair was prevented by the addition of translation inhibitors (LC condition). The fraction of full-length D1 degraded over 4 h was 53% in the wild type and 35% in *ftsh1-1*. When using the D1 DE loop antibody, we observed a similar increase in degradation of full-length D1 in the wild type as compared with the *ftsh1-1* mutant, with an additional 17% of full-length D1 being degraded in the wild type only. C-terminal epitopes recovered in

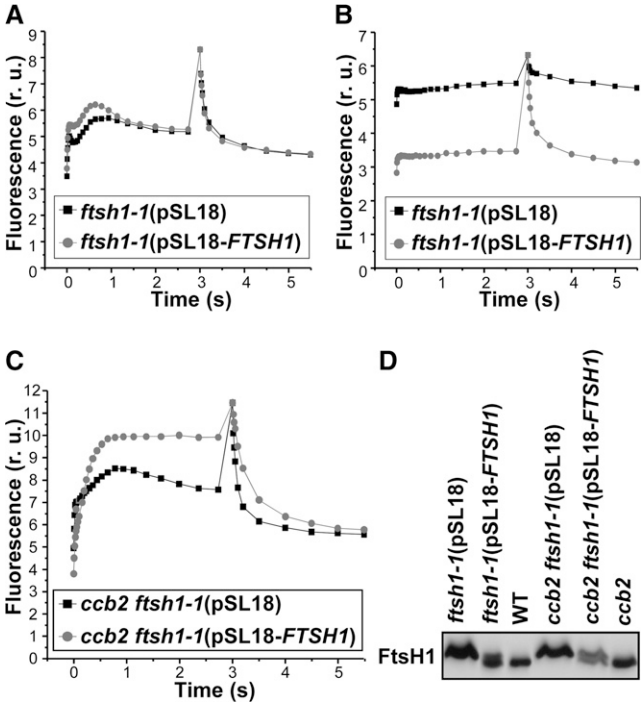

Figure 4. Complementation of *ftsh1-1* and *ccb2 ftsh1-1* Strains with *FTSH1* Genomic DNA Restores Wild-Type FtsH1 Phenotypes.

(A) Fluorescence induction kinetics in relative units (r.u.) at low actinic light of dark-adapted cells followed by a saturating pulse to determine F_m. Strains were grown at 6 μE m^{-2} s^{-1}.
(B) Fluorescence kinetics. Strains were grown at 6 μE m^{-2} s^{-1} followed by 19 h at 200 μE m^{-2} s^{-1}.
(C) Fluorescence kinetics. Strains were grown at 6 μE m^{-2} s^{-1}.
(D) Total cell proteins were separated on an 8% polyacrylamide gel in the presence of 8 M urea and analyzed by immunodetection with specific antibodies against FtsH1. Strains *ftsh1-1* and *ccb2 ftsh1-1* were complemented with *FTSH1* genomic DNA (pSL18-*FTSH1*) or as a control with empty pSL18 vector (pSL18).

D1 fragments amounted to 20% of total initial D1 (full-length plus fragments) in the *ftsh1-1* mutant, which indicates that D1 fragmentation was actively occurring in these experimental conditions. Thus, the defective activity of the FtsH protease impairs the degradation of damaged D1 and leads to some accumulation of D1 fragments. We note that the total amount of antibody-recognized C-terminal epitopes, borne by D1 full-length protein and fragments, decreased by 20% in the mutant in the LC condition, suggesting either that some degradation of the D1 C-terminal fragments still occurs or that there is some processive degradation of D1 that does not result in the production of D1 C-terminal fragments. A residual FtsH activity in the mutant may account for either of these two processes.

PSII Inactivation upon Phosphorus Starvation Is the Result of Enhanced Photoinhibition

Interestingly, impaired PSII activity also has been reported when *C. reinhardtii* is subjected to macronutrient stress, namely upon phosphorus and sulfur starvation (Wykoff et al., 1998; Zhang et al., 2002). In both cases, a loss of PSII proteins upon starvation was found responsible for PSII inactivation. The fact that the light intensity used in these experiments was ~80 μE m^{-2} s^{-1} suggested to us that a photoinhibitory effect might have developed, since macronutrient deprivation would lower the photosynthetic ability to fix carbon. If such was the case, we predicted that the *ftsh1-1* mutant, being unable to repair damaged D1, would be more sensitive than the wild type to these nutrient stresses and that PSII inactivation would only occur in the light.

We first subjected the *ftsh1-1* mutant to phosphorus starvation for 96 h either under illumination of 80 μE m^{-2} s^{-1} or in the dark. The cell response marker to phosphorus deprivation,

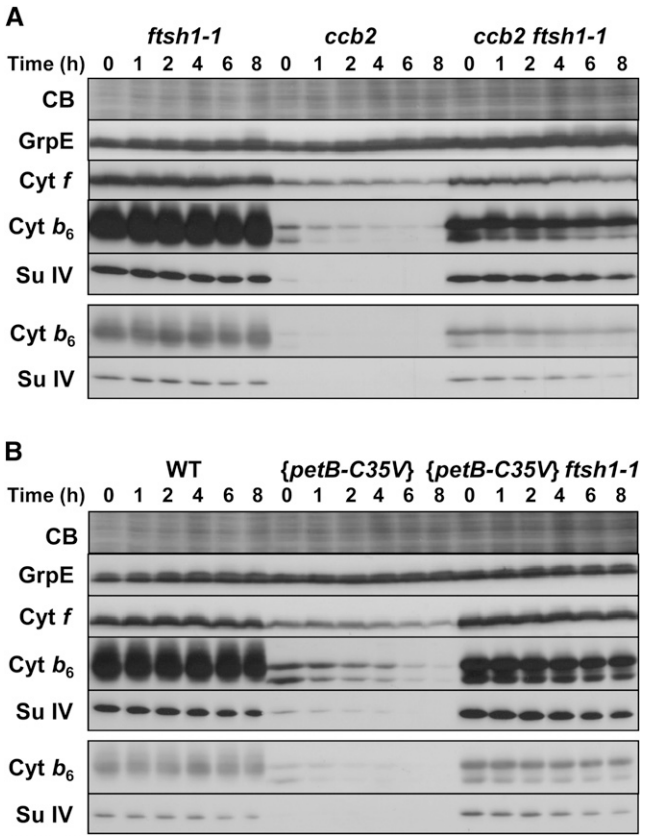

Figure 5. Accumulation and Lifetime of b_6f Complexes Lacking c_i Heme Are Highly Increased in the *ftsh1-1* Context.

(A) Immunochase of *ftsh1-1*, *ccb2*, and *ccb2 ftsh1-1* mutants. Immunochase was performed in the presence of 100 μg mL^{-1} chloramphenicol, an inhibitor of the translation of chloroplast genes. Total cell proteins were loaded at the chlorophyll constant, separated by SDS/urea-PAGE, and blotted onto a polyvinylidene difluoride membrane. The blot was stained with Coomassie blue (CB) and analyzed by enhanced chemiluminescence immunodetection with antibodies against cytochrome b_6f subunits and the nucleotide exchange factor GrpE.
(B) Immunochase of the wild type and the {*petB-C35V*} and {*petB-C35V*} *ftsh1-1* mutants in the same conditions as in **(A)**.
Note that for better comparison of the content in cytochrome b_6f subunits between mutants, shorter times of exposure of the immunoblots are shown at the bottom part of each panel.

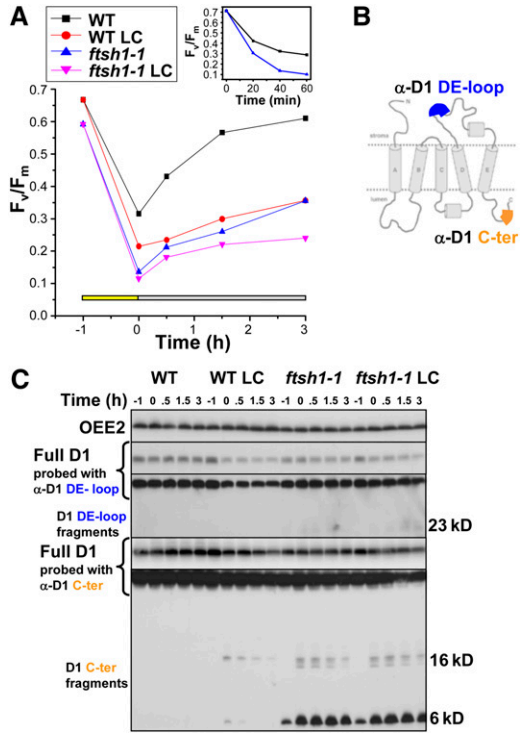

Figure 6. *ftsh1-1* Increases PSII Sensitivity to Photoinhibition, Prevents PSII Repair, and Leads to the Accumulation of D1 Fragments.

(A) Time course of photoinhibition at 250 μE m^{-2} s^{-1} and recovery at 6 μE m^{-2} s^{-1} in wild-type and *ftsh1-1* strains in the absence or presence of inhibitors of the translation of chloroplast genes (500 μg mL^{-1} lincomycin and 100 μg mL^{-1} chloramphenicol [LC]) as monitored by PSII activity (F_v/F_m). The inset shows kinetics of the PSII activity loss upon photoinhibition in an independent experiment.

(B) D1 model with the localization of the D1 DE loop and C-terminal peptides recognized by antibody (adapted from Kapri-Pardes et al., 2007).

(C) Time course of photoinhibition and recovery in wild-type and *ftsh1-1* strains as monitored by levels of D1 and D1 fragments immunodetected with D1 DE loop and C-terminal antibodies using the PSII OEE2 extrinsic subunit as a loading control. Total cell proteins were separated by SDS/urea-PAGE.

alkaline phosphatase (PHOX; Hallmann, 1999; Moseley et al., 2006), was induced in the light as well as in the dark in both the wild-type and *ftsh1-1* strains (top of Figures 7B and 7D). At 80 μE m^{-2} s^{-1}, the *ftsh1-1* mutant showed a more rapid and much larger loss in PSII activity than the wild type, as determined by their respective changes in F_v/F_m (Figure 7A) and a net decrease in the content of full-length D1 in the mutant at the late stage of starvation, probed with the D1 N-terminal antibody (Figure 7B, top). We then overexposed immunoblots reacted with D1 antibodies to the DE loop and C terminus to examine the pattern of accumulation of D1 fragments upon phosphorus starvation under 80 μE m^{-2} s^{-1} in the *ftsh1-1* mutated context. This pattern was similar to the one observed upon photoinhibition, showing an increased accumulation of D1 fragments, around 23 kD and in the 16- to 20-kD and 6- to 10-kD regions (Figure 7B). When phosphorus starvation was performed in the dark, both the *ftsh1-1* and wild-type strains preserved PSII activity over a period of 96 h (Figure 7C), and neither of them showed any accumulation of D1 fragments (Figure 7D). These results clearly demonstrate that compromised photosynthetic activity upon phosphorus starvation merely results from enhanced photoinhibition.

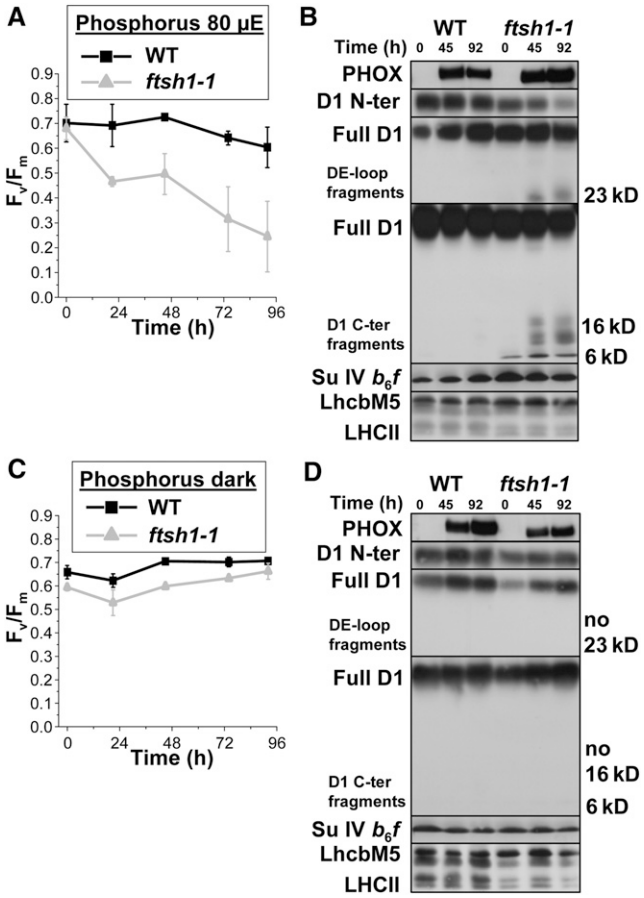

Figure 7. PSII upon Phosphorus Starvation in Wild-Type and *ftsh1-1* Strains.

(A) Time course of phosphorus starvation under 80 μE m^{-2} s^{-1} as monitored by PSII activity detection.

(B) Time course of phosphorus starvation under 80 μE m^{-2} s^{-1} as monitored by immunodetection of inducible PHOX (a marker of the cell response to phosphorus deprivation), full D1 and D1 fragments with D1 DE loop and C-terminal antibodies, cytochrome b_6f subunit IV, and light-harvesting LhcbM5. Total cell proteins were separated on a 7.5 to 15% polyacrylamide gel in the presence of 8 M urea.

(C) Time course of phosphorus starvation in the dark as monitored by PSII activity detection.

(D) Time course of phosphorus starvation in the dark as monitored by immunodetection.

Means and SD of two independent experiments for each starvation condition are given.

Compromised Photosynthetic Activity upon Sulfur Starvation under Illumination Is Due to Both Photoinhibition and Degradation of b_6f Complexes

When the *ftsh1-1* mutant was starved of sulfur under illumination of 80 μE m^{-2} s^{-1} over 96 h, it showed a larger PSII inactivation than the wild type (Figure 8A). This observation suggests, here again, an efficient FtsH-dependent repair process upon sulfur starvation of *C. reinhardtii* wild-type cells, similar to the repair upon photoinhibition. Indeed, the decrease in D1 content during sulfur starvation was far more pronounced in the mutant than in the wild type (Figure 8B).

However, there were marked differences with regard to phosphorus starvation or a regular photoinhibition process: the cytochrome b_6f complex, as probed with an antibody against the Rieske protein subunit, was now targeted to degradation in the two strains, and the drastic degradation of full-length D1 in the *ftsh1-1* mutant was accompanied by a transient overaccumulation of D1 fragments at 21 h of starvation, which were subsequently disposed of. Whereas at a late stage of sulfur starvation there was a general decrease in protein content in the mutant, as shown by the decreased content in the cell response marker to sulfur deprivation, SLT2 (Pootakham et al., 2010), and the β-subunit of CF1 (Figure 8B), we noted that the other subunits of the PSII core, D2 and CP47, better resisted degradation than D1. This result raised the question of whether D2 and CP47 were in a disassembled state or perhaps still assembled with fragmented D1 in the *ftsh1-1* mutant. We assayed this hypothesis by two-dimensional BN/SDS-PAGE of dodecyl-maltoside–solubilized membranes isolated after 39 h of sulfur starvation (Figure 8E, bottom). We found that fragmented D1 remained assembled within PSII monomers and reaction center cores lacking CP43 (RC47) in the *ftsh1-1* mutant. This finding is in line with what has been reported for the *Arabidopsis* FtsH2 (*var2*) mutant after 1 h of extreme high-light exposure at 2500 μE m^{-2} s^{-1} (Kato et al., 2012). We note that, before starvation, PSII supercomplexes were far more abundant in the wild type than in the *ftsh1-1* strain (Figure 8E, top), as also was suggested by the analysis of digitonin-solubilized membranes (Figure 3D).

We also examined the behavior of the wild type and the *ftsh1-1* mutant when sulfur starvation was performed in photoautotrophic conditions, under an illumination of 80 μE m^{-2} s^{-1} in the absence of the carbon source acetate. Both strains showed a delayed loss in PSII activity and downstream electron transfer (Supplemental Figures 7A to 7D). They also showed a retarded induction of the sulfate transporter SLT2, probably due to their slower growth and lower sulfur consumption in minimal medium (Supplemental Figures 7E and 7F).

The *ftsh1-1* Mutant Conserves Most PSII and b_6f Complexes upon Sulfur Starvation in the Dark, in Contrast to the Wild-Type Strain

To further understand to what extent photoinhibitory processes contributed to the loss of PSII upon sulfur starvation, we performed the same starvation experiments in complete darkness. To our surprise, wild-type cells showed a more dramatic inactivation of PSII (Figure 8C), which was now accompanied by a net loss of D1 and D2 proteins. Thus, the repair process that was efficient in the light (Figures 8A and 8B) was either heavily compromised in the dark or unable to make up for higher rates of PSII degradation (Figures 8C and 8D). That the process of PSII degradation in the dark was widely different from the one operating under illumination was demonstrated by the behavior of the *ftsh1-1* mutant, which preserved fully active PSII when starved of sulfur in the dark (Figures 8C and 8D). SLT2 was induced upon sulfur depletion in the dark in the two strains, indicating that the differences in PSII degradation should not be attributed to an absence of signaling of sulfur deficiency in the *ftsh1-1* mutant. The cytochrome b_6f complexes were degraded in the wild type starved of sulfur in the dark, as they were under 80 μE m^{-2} s^{-1}, but this degradation in the dark was now largely FtsH dependent, since the *ftsh1-1* mutant showed very limited cytochrome b_6f degradation in contrast to its behavior in the light (Figures 8B and 8D).

The accumulation pattern of D1 fragments upon sulfur starvation of the *ftsh1-1* mutant in the dark also differed from the one observed upon photoinhibition, with an absence of 23-kD fragments (Figure 8D). This is consistent with the previously characterized light-induced production of a 23-kD D1 fragment as a substrate of the thylakoid FtsH protease (Lindahl et al., 2000). Importantly, the 6- to 10-kD and 16- to 20-kD fragments still accumulated in the dark. We also note that sulfur starvation induced extensive accumulation of D1/D2 oligomers of high molecular weight in the dark but not in the light in the *ftsh1-1* mutated context only (Supplemental Figure 8).

Finally, we tested whether increased expression in some other major chloroplast proteases would have occurred upon FtsH inactivation, which would explain the more pronounced PSII degradation in the *ftsh1-1* mutant upon sulfur deprivation in mixotrophic conditions. We used antibodies against FtsH1/FtsH2, stromal ClpP1, lumenal Deg5, and stromal membrane–associated SppA1 to probe the content of major chloroplast proteases in wild-type and *ftsh1-1* cells starved of sulfur in the presence or absence of acetate (Supplemental Figures 7E and 7F). The patterns of accumulation were rather similar for the two strains, indicating that there was no upregulation of the probed proteases in the FtsH-defective mutant. Sulfur starvation caused a rapid loss in Deg5 and ClpP1 in the two strains and some processing of SppA1 in mixotrophic conditions only. FtsH and SppA1 were better preserved than Deg5 and ClpP1 when sulfur starvation was performed in the absence of acetate, especially in the *ftsh1-1* mutant (Supplemental Figure 7F).

The *ftsh1-1* Mutation Has a Limited, if Any, Ability to Prevent the Degradation of Unassembled Subunits from the Cytochrome b_6f Complex or the PSII Protein Complex

A concerted accumulation of PSII subunits that make up an active PSII protein has been demonstrated to result from a posttranslational regulation leading to the proteolytic disposal of unassembled subunit D2 and CP43 and a downregulation of the translation of subunit D1 or CP47, which are control by epistasy of synthesis (CES) subunits (de Vitry et al., 1989; Minai et al., 2006). We crossed the *ftsh1-1* nuclear mutant to chloroplast mutants with a deleted *PsbC* (CP43) gene or harboring a premature stop codon in *PsbA* that leads to the expression of

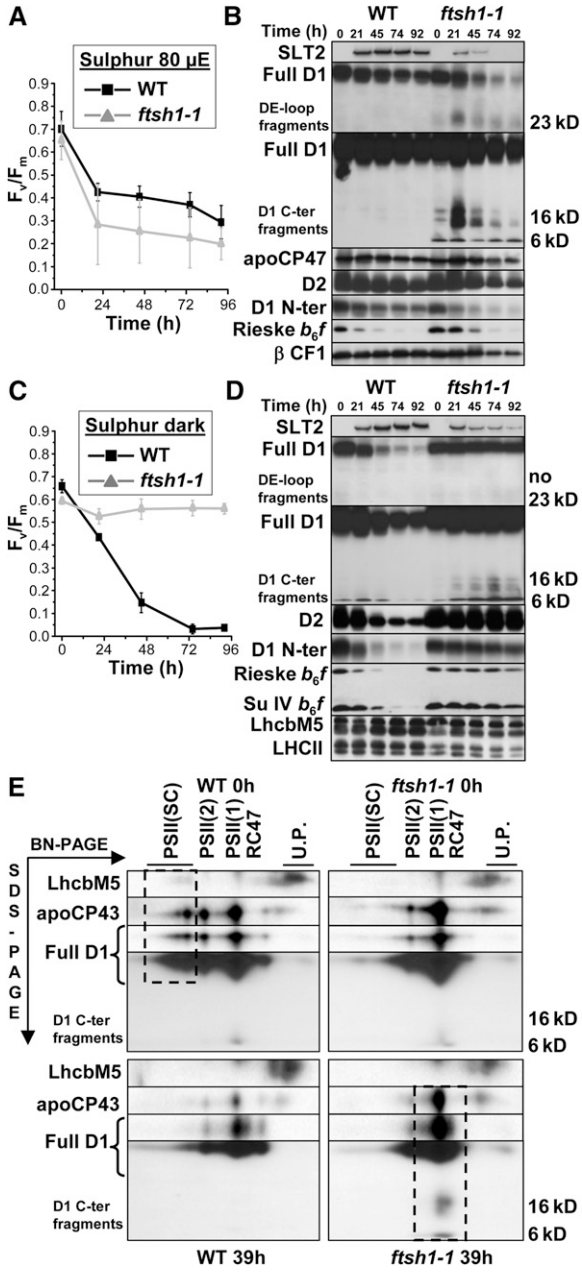

Figure 8. PSII and Cytochrome b_6f upon Sulfur Starvation in Wild-Type and *ftsh1-1* Strains.

(A) Time course of sulfur starvation under 80 µE m^{-2} s^{-1} as monitored by PSII activity detection.

(B) Time course of sulfur starvation under 80 µE m^{-2} s^{-1} as monitored by immunodetection of a cell response marker to sulfur deprivation (sulfate transporter SLT2) and of PSII subunits (D1, D2, and CP47), cytochrome b_6f subunits (IV and Rieske), and light-harvesting LhcbM5. Total cell proteins were separated as in Figure 7.

(C) Time course of sulfur starvation in the dark as monitored by PSII activity detection.

(D) Time course of sulfur starvation in the dark as monitored by immunodetection.

(E) PSII complexes after BN-PAGE of dodecyl-maltoside–solubilized membranes at 0 and 39 h of sulfur deprivation under 80 µE m^{-2} s^{-1} were separated by two-dimensional BN (3 to 12%)/SDS-PAGE (12% in the presence of 8 M urea), blotted onto a polyvinylidene difluoride membrane, and immunodetected. The positions of unassembled proteins (U.P.), a reaction center core lacking CP43 (RC47), and monomers [PSII(1)], dimers [PSII(2)], and supercomplexes [PSII(SC)] of PSII are indicated. At 0 h, supercomplexes are more abundant in the wild-type than in *ftsh1-1*; at 39 h, fragmented D1 was found assembled in monomeric PSII and RC47 complexes in the *ftsh1-1* mutant (dashed boxes).

Means and SD of two independent experiments for each starvation condition are given.

a truncated and labile D1. We found no evidence that the mutation *ftsh1-1* rescued the accumulation of the other PSII subunits when PSII assembly was compromised in these mutants (Supplemental Figure 9). To assess whether this protease also determines the lifetime of unassembled subunits of the cytochrome b_6f complex, most of which are subjected to rapid degradation, with the exception of cytochrome *f*, which is a CES subunit (Kuras and Wollman, 1994; Choquet et al., 1998), we tested whether the mutation *ftsh1-1* rescues the accumulation of cytochrome b_6 in the absence of cytochrome *f* and vice versa. To this end, we crossed the nuclear *ftsh1-1* mutant with chloroplast mutants lacking either the *petA* gene, encoding cytochrome *f*, the *petA* and *petD* genes, the latter encoding subunit IV, or the *petB* gene, encoding cytochrome b_6. The accumulation of unassembled cytochrome b_6 showed a limited but noticeable increase in an FtsH-defective context (Figure 9A), whereas unassembled cytochrome *f*, whose decreased accumulation is due to a decreased translation initiation according to the CES process, proved, as expected, insensitive to the status of the FtsH protease (Figure 9B). In these experiments, the level of accumulation of subunit IV in the absence of its assembly partners remained below detectable levels.

DISCUSSION

The Thylakoid FtsH Protease of *C. reinhardtii* Forms Heterooligomers Comprising FtsH1 and FtsH2

The *C. reinhardtii* nuclear genome encodes six members of the FtsH family distributed between the mitochondria (Atteia et al., 2009) and the chloroplast and three FtsH-like proteins (FHL1 to FHL3) that retain a complete AAA+ domain but lack the zinc binding motif (reviewed in Schroda and Vallon, 2009; see phylogenetic tree of FtsH proteins in Supplemental Figure 1). Only two isoforms have been identified in *C. reinhardtii* thylakoid membranes: FtsH1 (type A) and FtsH2 (type B; Allmer et al., 2006). Our two-dimensional BN/SDS-PAGE and coimmunoprecipitation experiments demonstrate that FtsH1 also forms heterocomplexes with FtsH2 in *C. reinhardtii* (Figures 3D and 3E). FtsH(L), however, has a much larger apparent molecular mass than expected for a heterohexamer (~410 kD, to which should be added a digitonin contribution that has a micellar mass of ~70 kD). Such large FtsH-containing complexes, around or above 1 MD, were previously observed in *E. coli*, yeast mitochondria, and *Arabidopsis* mitochondria, where they also include prohibitin-like proteins whose function remains

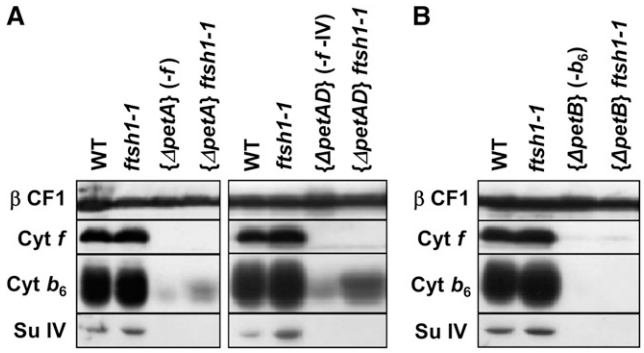

Figure 9. The Accumulation of Cytochrome b_6 Lacking Assembly Partners Shows a Limited but Noticeable Increase in an FtsH-Defective Context.

(A) Double mutants obtained by crosses of the nuclear *ftsh1-1* mutant with chloroplast mutants deleted for either the *petA* gene, encoding cytochrome *f*, or the *petA* and *petD* genes, the latter encoding subunit IV, accumulated more cytochrome b_6 when cytochrome *f* was missing than the {Δ*petA*} and {Δ*petAD*} mutants. Total cell proteins were separated by SDS/urea-PAGE and analyzed by immunodetection with antibodies against cytochrome b_6f subunits (cytochrome *f*, cytochrome b_6, and subunit IV) and the ATP synthase β-subunit (β CF1) as a loading control. **(B)** Unassembled cytochrome *f* when cytochrome b_6 is missing, as in the {Δ*petB*} mutant context, was insensitive to the presence of the *ftsh1-1* mutation.

unclear (Steglich et al., 1999; Saikawa et al., 2004; Piechota et al., 2010). Similar high molecular mass FtsH-containing complexes were described in *Synechocystis* (Boehm et al., 2012) with a transient or detergent-sensitive association with prohibitin-like proteins (Boehm et al., 2009). Thus, the thylakoid enzyme from *C. reinhardtii* shows a similar but simpler subunit composition than its counterpart from *Arabidopsis*, which assembles four distinct FtsH isoforms. We cannot exclude that some FtsH1 and/or FtsH2 may form homohexamer complexes, although homomeric structures are thought to be less likely to exist since they are less stable, as modeled by Moldavski et al. (2012).

The *ftsh1-1* Mutation Largely Impairs FtsH Olimerization and Should Affect ATP Hydrolysis in the *C. reinhardtii* FtsH Protease

Here, we generated, by a genetic suppressor approach, an FtsH mutant in *C. reinhardtii*, which we named *ftsh1-1*. It carries a mutation in the *FtsH1* gene that substitutes a well-conserved Arg, Arg-420, in the SRH domain by a Cys residue (Figures 3A and 3B). Arg-420 was first proposed to form an Arg finger (Karata et al., 1999), which should coordinate the γ-phosphate of a bound ATP and contribute to its hydrolysis through stabilization of the transition state of the reaction, as described in GTPase-activating proteins (Ahmadian et al., 1997). Indeed, several mutations of the two SRH-conserved Arg residues in *E. coli* were shown to compromise ATP hydrolysis and thereby protease activity (Karata et al., 1999, 2001). Arg-420 from *C. reinhardtii* corresponds to the second SRH-conserved Arg, Arg-315, in *E. coli*, which was proposed to be located at hydrogen bonding distance of the γ-phosphate of bound ATP to the adjacent subunit in the dimeric crystal structure of the apoFtsH AAA domain of *E. coli* (Krzywda et al., 2002; Ogura et al., 2004). However, in the hexameric crystal structures of ADP-FtsH lacking the transmembrane domain, it is the other conserved Arg, FtsH1-R417 in *C. reinhardtii*, that was proposed to form an Arg finger in the thermophilic bacterium *Aquifex aeolicus* (Suno et al., 2006), while the conserved Arg residue corresponding to *C. reinhardtii* FtsH1-R420 is localized at the intersubunit interface, where it could contribute to the oligomerization of the enzyme by its participation in a salt bridge with a conserved Asp residue from the same subunit in the thermophilic bacterium *Thermotoga maritima* (Bieniossek et al., 2006).

Indeed, the *ftsh1-1* mutant still displays wild-type amounts of the two FtsH isoforms (Figure 3C) with an altered oligomerization pattern (Figure 3D). We observed, however, a well-preserved interaction between FtsH1 and FtsH2, as shown by coimmunoprecipitation (Figure 3E). The striking increase in the proportion of FtsH1 and FtsH2 found in FtsH(S) in the *ftsh1-1* mutant (Figure 3D) is consistent with an accumulation of FtsH1/FtsH2 heterodimers due to the location of the mutation at the intersubunit interface. This Arg/Cys amino acid substitution would loosen the formation of the FtsH hexamers and hamper their integration with partner proteins, or substrates, in larger heterooligomers, resulting in a higher yield of FtsH heterodimers. As the ClpX hexameric unfoldase of the AAA+ protein family was shown to retain some function even if only one subunit could hydrolyze ATP (Martin et al., 2005), ATP hydrolysis by wild-type FtsH2 subunits in *ftsh1-1* heterocomplexes may allow some digestive power. We conclude that these changes in oligomerization and probably also in ATP hydrolysis deeply affect the protease and unfoldase activities, leading to a lower quality control of partially assembled or misassembled complexes that are particularly difficult to unfold.

Degradation of Unassembled Subunits from the Cytochrome b_6f Complex or the PSII Protein Complex Still Occurs with High Efficiency in the *ftsh1-1* Mutated Context

The above conclusion that the *ftsh1-1* mutation may prevent the unfolding of substrates for degradation rather than proteolysis itself is consistent with its very limited effect on the accumulation level of unassembled subunits from the cytochrome b_6f complex and the PSII complex. For instance, D2 and CP43 showed no increased accumulation when the *ftsh1-1* mutation was introduced in a strain showing premature termination of D1 that prevents PSII core assembly (Supplemental Figure 9B), thus leading to proteolytic disposal of these subunits (Minai et al., 2006). Similarly, subunit IV was still efficiently degraded in the *ftsh1-1* mutated context whether cytochrome *f* or cytochrome b_6 was missing (Figure 9). We noted, however, some increase in the accumulation of unassembled cytochrome b_6 when the activity of FtsH was compromised, which suggests that unfolding of holocytochrome b_6 may facilitate its degradation (Figure 9A). However, the *ftsh1-1* mutant did not show any increase in the accumulation of the partially assembled PSII subcomplex D2/D1/CP47 in a mutant lacking CP43 (Supplemental Figure 9A), which is at variance with the effect of a knockout of the FtsH gene (slr0228) in *Synechocystis*, which stabilized various PSII assembly

intermediates in PSII mutants lacking CP43 or impaired in the assembly or stability of the manganese cluster (Komenda et al., 2006, 2010). Although we cannot fully exclude a residual FtsH activity that would degrade these unassembled, or partly assembled, subunits in the *ftsh1-1* mutated context, we tentatively attribute these differences to the lower protein quality control in cyanobacterial thylakoid membranes when compared with *C. reinhardtii* chloroplasts (Wollman et al., 1999). In particular, crippled PSII complexes are less efficiently degraded in *Synechocystis* (de Vitry et al., 1989; Vermaas, 1998) than in photosynthetic eukaryotes. These observations suggest the presence of an as yet unidentified additional housekeeping protease that degrades these subunits in the thylakoid membranes of *C. reinhardtii*.

FtsH Is Involved in Quality Control and the Regulation of Accumulation of Cytochrome b_6f Complexes and CCB Proteins

The first suggestion of a cytochrome b_6f subunit degraded by FtsH was the unassembled Rieske iron-sulfur protein imported into isolated chloroplasts in vitro (Ostersetzer and Adam, 1997). The involvement of FtsH in cytochrome b_6f degradation in vivo is demonstrated here with the identification of the *ftsh1-1* mutant by the present genetic suppressor strategy. In marked contrast to the continued degradation of the cytochrome b_6f subunits when a subunit is absent (Figure 9), a diversity of labile c_i heme–deficient cytochrome b_6f complexes proved resistant to degradation in the *ftsh1-1* mutated context. They ranged from site-directed substitution of the Cys involved in the binding of the c_i heme (Figure 5) to site-directed substitution of the His ligand of the b_h heme (Malnoë et al., 2011) and to mutants in the CCB heme binding pathway (Figure 2). These observations demonstrate that FtsH operates as a major quality control protease that recognizes altered conformations in cytochrome b_6f assemblies to trigger their degradation through the combined action of its unfoldase and proteolytic activities. A similar situation may prevail in *Saccharomyces cerevisiae* mitochondria, where FtsH proteases with the catalytic site facing the matrix (m-FtsH) Yta10/Yta12 have been described as involved in maturase-dependent intron splicing of cytochrome *b* transcripts. However, when using an intronless mitochondrial genome where cytochrome *b* synthesis was not affected, m-FtsH was shown to contribute to posttranslational bc_1 complex assembly and degradation (Guzélin et al., 1996; Arlt et al., 1998; Van Dyck and Langer, 1999). As we report here for sulfur starvation (Figures 8B and 8D) and elsewhere for nitrogen starvation (Bulté and Wollman, 1992; Wei et al., 2013), FtsH has a prominent role in regulating the accumulation level of cytochrome b_6f complexes upon these macronutrient stresses in low light or in the dark.

We also found that degradation of unassembled CCB4 in the absence of CCB2 (and vice versa), both of which are transmembrane proteins involved in the c_i heme binding pathway to cytochrome b_6 (Saint-Marcoux et al., 2009), proved to be regulated by FtsH (Figure 1B), in line with our report elsewhere (Wei et al., 2013) of a global role for FtsH in the degradation of photosynthetic complexes and their assembly factors.

The ClpP protease also has been demonstrated to play a role in cytochrome b_6f degradation in *C. reinhardtii* (Majeran et al., 2000), as does Deg1 on cytochrome b_6 in *Arabidopsis* (Zienkiewicz et al., 2012). However, Clp and FtsH may have distinct actions on the degradation of cytochrome b_6f complexes, since a Clp-deficient mutant was unable to protect b_6f complexes from degradation in mutants lacking c_i heme (Majeran et al., 2000), while the *ftsh1-1* mutation did so (Figure 5).

Here, we observed a cytochrome b_6f degradation process that was selectively activated in sulfur-deficient conditions. Cytochrome b_6f was degraded in the light but not in darkness in the *ftsh1-1* mutant, suggesting the action of some additional protease upon illumination. Steady state levels of the chloroplast proteases that we probed, including ClpP1 and Deg5, were rather reduced upon sulfur starvation in the light, but we cannot rule out that some proteases might have better access to cytochrome b_6f or be activated by oligomerization in the light in these starvation conditions.

FtsH1 Regulates the Degradation of PSII upon Photoinhibition and Phosphorus and Sulfur Starvation

In cyanobacteria, FtsH has mainly been studied for its role in D1 degradation (reviewed in Nixon et al., 2010; Komenda et al., 2012) and the removal of other damaged or unassembled PSII proteins (Komenda et al., 2006, 2010; Boehm et al., 2011). In one study, FtsH was also shown to contribute to the regulation of PSI amounts (Mann et al., 2000). The mechanism for D1 protein degradation is not fully elucidated, but it is known to involve the reaction of damaging reactive oxygen species, partial disassembly of the PSII complex to form the RC47 complex, and the action of several proteases, notably FtsH, that selectively remove damaged D1 (reviewed in Edelman and Mattoo, 2008; Komenda et al., 2012). The best-documented function of FtsH in thylakoid membranes is in this PSII repair cycle (reviewed in Kato and Sakamoto, 2009). A model for the photoinhibition of cyanobacteria has been proposed in which damaged D1 is removed by FtsH heterohexamers, with degradation proceeding from the N terminus of D1 in a highly processive manner without the requirement of any other proteases (reviewed in Nixon et al., 2010). In particular, photoinhibition studies with the Δ*htrA*/*hhoA*/*hhoB* triple mutant, defective for the three genes encoding Deg proteases in *Synechocystis* sp PCC6803, showed that Deg proteases are not required for the removal of damaged D1 protein during the PSII repair cycle when exposed to high light intensity (Barker et al., 2006). These results are in contrast to several photoinhibition studies performed with *Arabidopsis* showing that PSII protein turnover required both the involvement of FtsH and Deg/Htr proteases (Itzhaki et al., 1998; Kapri-Pardes et al., 2007; Sun et al., 2007). High-light treatment was reported to increase the expression of Deg/Htr and FtsH types of proteases in *Arabidopsis* (Sinvany-Villalobo et al., 2004), to raise the level of FtsH hexamerization and unstacking of thylakoids (reviewed in Yoshioka and Yamamoto, 2011), and to activate the lumenal Deg protease, based on in vitro experiments showing its hexamerization upon acidification (Kley et al., 2011). Thus, a model for D1 degradation in the chloroplast was proposed in which Deg proteases act as

endoproteases fragmenting D1 and FtsH proteases act as exoproteases processively degrading D1 and its fragments (reviewed in Kato and Sakamoto, 2009). The reason why cyanobacterial FtsH would be capable of processive degradation of the whole D1 protein from the stromal side, while the ability of its homolog in the chloroplast is far reduced, may rest in the difference in subunit composition of FtsH from the two types of organisms as well as from the embedment of chloroplast D1 in grana membranes, where it has increased interaction with transmembrane antenna proteins and lumenal oxygen-evolving enhancer subunits (for further discussion, see Edelman and Mattoo, 2008).

Here, in agreement with previous photoinhibition studies from vascular plant chloroplasts and cyanobacteria, we showed that the *ftsh1-1* mutation increased PSII sensitivity to photoinhibition and impaired proteolytic degradation and replacement of D1 by a de novo synthesized copy (Figure 6). There is a striking similarity in the fate of D1 in the *ftsh1-1* mutant when subjected to light stress or phosphorus starvation under moderate illumination, both of which lead to PSII inactivation in *C. reinhardtii* (Wykoff et al., 1998; Zhang et al., 2002). Here, we have demonstrated that, indeed, compromised photosynthetic activity upon phosphorus starvation was mainly due to enhanced photoinhibition (Figure 7). In contrast, PSII inactivation upon sulfur starvation cannot be attributed solely to photoinhibition, since it develops even more strongly when sulfur starvation is performed in complete darkness. Since PSII inactivation and D1 degradation in the *ftsh1-1* mutant are markedly increased upon sulfur starvation in the light but fully prevented when performed in darkness (Figure 8), one could consider a light-induced upregulation of ClpP when FtsH activity is defective, as recently demonstrated (Kato et al., 2012). Although we did not detect more ClpP in *ftsh1-1* than in the wild-type strain in these conditions (Supplemental Figure 7E), we cannot exclude an upregulation of ClpP activity through changes in its state of oligomerization, substrate accessibility, or ATP availability.

FtsH1 Regulates the Degradation of PSII by Removing D1 Fragments

A clear consequence of the inactivation of FtsH in the *ftsh1-1* mutant was the detection of D1 fragments upon photoinhibition, which suggests that primary endoproteolytic cuts occurred in the mutant but that their processive degradation by FtsH was inhibited (Figure 6C). According to what has been proposed for plant chloroplasts, there could be a joint action of Deg and FtsH proteases in the degradation and repair of D1 upon photoinhibition of *C. reinhardtii*. Indeed, the set of chloroplast Deg proteases is similar in *Arabidopsis* (lumenal Deg1, Deg5, and Deg8 and stromal Deg2, Deg6, Deg7, Deg9, and Deg16) and in *C. reinhardtii* (lumenal Deg1A, Deg1B, Deg1C, Deg5, and Deg8 and stromal Deg2, Deg7, and Deg9; Huesgen et al., 2009; Schroda and Vallon, 2009; Sun et al., 2010). The model of Kato and Sakamoto (2009), derived from studies with *Arabidopsis*, predicts the production of Deg-dependent fragments whose apparent molecular mass and epitope content match nicely to those we detected with the two distinct D1 antibodies we used (Supplemental Figure 10).

The physiological significance of the Deg-dependent D1 degradation pathway has been under debate (for discussion, see Edelman and Mattoo, 2008; Komenda et al., 2012). Is it synergistic with FtsH, or is it an escape pathway that supplements the FtsH-mediated one to accelerate D1 degradation under photoinhibitory conditions? We conclude that in our experimental conditions, when the function of FtsH is impaired, the Deg pathway would be rather active, with 20% of the C-terminal epitopes of D1 being found in its fragments (Figure 6C).

We note, however, that most of these fragments accumulated to a limited extent. This could be due to a negative feedback inhibition of the Deg proteases by the accumulation of these early D1 degradation products whose stroma-exposed domains are not processed by FtsH. This is consistent with the observation that the only degradation product that accumulates extensively in the *ftsh1-1* mutant is in the ~6-kD region, where the C-terminal fragment of D1, which is lumen localized, should be found. This fragment differs from all the others in that it should never have access to the stroma-located proteolytic chamber of FtsH in a wild-type context and, therefore, should not be degraded by FtsH. Its increased production in the *ftsh1-1* mutant, as compared with the wild type, probably results from the slower digestion of D1 products by FtsH, thus releasing more 6-kD fragments in the lumen.

A conspicuous feature of the various PSII degradation processes upon macronutrient starvation, whether it be phosphorus or sulfur starvation under moderate illumination or sulfur starvation in the dark, is the production of D1 fragments in the *ftsh1-1* mutated context. With the exception of the 23-kD fragment, which is detected only upon illumination and serves as a diagnostic of photoinhibition, as suggested previously (Lindahl et al., 2000), the D1 fragmentation patterns upon macronutrient stress (Figures 7B, 8B, and 8D) are very similar to one resulting from photoinhibition (Figure 6C), with a group of fragments accumulating in the 16- to 20-kD and 6- to 10-kD regions. These observations strongly suggest a contribution of the Deg protease family to the degradation of D1 upon nutrient stress as they do upon photoinhibition. Indeed, Degs were also proposed to contribute to D1 degradation under stress conditions by cleaving cross-links to neighboring proteins (Komenda et al., 2012). A modest expression increase in lumenal Deg1C in *C. reinhardtii* has been found upon phosphorus and sulfur starvation (Zhang et al., 2004; Moseley et al., 2006), and a 3-fold increase of the transcript level of stromal Deg2 upon sulfur starvation in the light in the wild-type strain was also observed (González-Ballester et al., 2010). Here, however, we detected a net decrease of the amount of chloroplast proteases upon sulfur depletion in the presence of acetate (Supplemental Figure 7E). In the latter experimental conditions, D1 fragments transiently overaccumulate in the *ftsh1-1* mutant (Figure 8B), which supports a degradation pathway in which Deg proteases produce a first set of early endoproteolytic cuts that can be continued only once the resulting D1 fragments are themselves degraded by processive proteases such as FtsH.

It is of note that light-induced oxidative damage to D1 should not be considered as a prerequisite for the activation of its degradation by the combined effects of FtsH and Deg proteases, since D1 degradation yields the same 16- to 20-kD and 6- to 10-kD fragments when operating in the dark in sulfur stress conditions (Figure 8D). However, the activation of the Deg proteases in the lumen has been shown to be triggered by the high

ΔpH formed in the light (Kley et al., 2011). How they are activated in the dark remains unclear unless a high proton gradient is present during sulfur starvation in the dark, an issue that needs to be addressed in the future.

Enhanced Degradation of PSII upon Sulfur Starvation in the Dark Is Fully FtsH Dependent

That PSII degradation was dramatically enhanced when sulfur starvation was performed in the dark was unexpected (Figure 8D). In this case, PSII degradation became a fully FtsH-dependent process. The rationale for this targeted degradation of PSII in darkness upon sulfur starvation remains unclear. It is not a consequence of functional damage to PSII complexes, since the *ftsh1-1* mutant, which does not degrade PSII, displays a fluorescence pattern with a high F_v/F_m typical of active PSII centers (Figure 8C). It should not be aimed either at scavenging sulfur, since most of the sulfur-containing cofactors for photosynthesis are found within PSI and not in association with PSII. Interestingly, we noted a spectacular increase in the accumulation of D1/D2 oligomers in the *ftsh1-1* mutant relative to the wild type when deprived of sulfur in the dark (Supplemental Figure 8). Similar cross-linking products or adducts had been reported previously either during a light stress or in the dark when a heat or oxidative stress was applied (reviewed in Yamamoto et al., 2008). The accumulation of these oligomers in the dark during a nutrient stress is highly unusual and raises the question of how they are formed. These oligomers may be the privileged substrate for PSII degradation by FtsH upon sulfur stress in the dark. Being resistant to other proteases, they might be a form of active PSII, which is worthy of further investigation.

The mechanism of activation of this degradation pathway is unknown and might be related to sulfur stress–induced expression of chaperones. Indeed, it has been shown in *E. coli* that chaperones can facilitate degradation by FtsH (Rodriguez et al., 2008). The chloroplast DnaJ chaperone Atg8, induced in darkness and stabilized by FtsH (Chen et al., 2011), is thus a good candidate for being involved in the dark-activated and FtsH-dependent degradation of PSII upon sulfur deprivation.

METHODS

Phylogenetic Analysis

Multiple sequence alignment was performed using ClustalW2.1 (Larkin et al., 2007) with default parameters followed by manual editing. After removing ambiguously aligned N- and C-terminal regions, 639 sites were retained for the phylogenetic analysis (Supplemental Data Set 1). The best-fit amino acid substitution model was determined using ProtTest2.4 (Abascal et al., 2005). The best-fit model was the Le-Gascuel model (Le and Gascuel, 2008) supplemented with a γ distribution for rate variations among sites (LG+G). The tree was reconstructed by the maximum likelihood method based on the LG+G model using RaxML7.2.6 (Stamatakis, 2006). Statistical support for nodes was assessed with 1000 bootstrap replicates.

Chlamydomonas reinhardtii Strains, Growth Conditions, and Genetic Methods

C. reinhardtii mutants have been described previously and were as follows: *ccb*, {*petB-C35V*}, {*petB-H202Q*}, {*petB-H187G*}, {Δ*petB*}, {Δ*petA*}, {*Fud34*}, {*Fud7*}, {*D1TR*}, *arg7*, and *arg2* (Eversole, 1956; Matagne, 1978; de Vitry et al., 1989, 2004; Kuras and Wollman, 1994; Kuras et al., 1997, 2007; Minai et al., 2006). Cells were grown at 25°C in Tris-acetate-phosphate (TAP) medium or, when indicated, in minimal medium lacking acetate, pH 7.2, under dim light at 6 μE m^{-2} s^{-1} and collected during the exponential phase at 2 × 10^6 cells mL^{-1}. Plasmid pΔ*petA-D* was constructed by ligating the *Sca*I-*Pst*I fragment of 4296 bp of plasmid pΔ*petA* (Kuras and Wollman, 1994) bearing the Δ*petA* deletion with the *Sca*I-*Pst*I fragment of 2134 bp of plasmid pK*f*Δ*petD* (Choquet et al., 2003) bearing the Δ*petD* deletion and containing the *aadA* cassette conferring spectinomycin resistance. Plasmid pΔ*petA-D* was transformed by the biolistic method into *C. reinhardtii* wild-type strain (Boynton et al., 1988; Kuras and Wollman, 1994). Nonphotosynthetic {Δ*petAD*} transformants were screened in the dark on TAP-agar-spectinomycin medium, and homoplasmy was checked by RNA gel blotting for the absence of *PETA* and *PETD* mRNA as described (Drapier et al. 2002) with probes derived from coding sequences (Eberhard et al., 2002). UV light mutagenesis on *ccb* strains to obtain phototrophic revertants was performed as described (Li et al., 1996). Plasmid pSL18-*FTSH1* was constructed by ligating the *Nde*I/*Xba*I-digested fragment of 3.5 kb (partially digested to avoid cutting the *Nde*I site in FtsH1g) of the amplified PCR-coding phase of FtsH1 genomic DNA, adding the *Nde*I site before and the *Xba*I site after the coding sequence, with the *Nde*I/*Xba*I-digested fragment of 6069 bp of vector pSL18 (Depège et al., 2003) carrying an expression cassette composed of the *PSAD* promoter and polyadenylation site and a paromomycin resistance cassette. Plasmids pSL18-*FTSH1* and pSL18 were transformed by the electroporation method (Shimogawara et al., 1998) into *C. reinhardtii ftsh1-1* and *ftsh1-1 ccb2* mutants. Transformants were screened on TAP-agar-paromomycin medium in the presence of 10 μg mL^{-1} paromomycin and analyzed by fluorescence; the expression of wild-type FtsH1 was checked by immunodetection. Crosses were performed and vegetative diploids were isolated according to published protocols (Harris, 1989).

Map-Based Cloning of $Su_{1\text{-}ccb2}$

The *C. reinhardtii* $Su_{1\text{-}ccb2}$ mutant was crossed with the interfertile species *Chlamydomonas grossii*, which shows suitable profusion of genomic polymorphism (Rymarquis et al., 2005). In each of 127 tetrads, we took one progeny carrying the $Su_{1\text{-}ccb2}$ mutation, as identified by its photosensitivity, for linkage analysis to various markers by a PCR method. The primers were used in a single reaction and generated PCR products that differ in size for the *C. reinhardtii* or the *C. grossii* allele and were assayed directly on an agarose gel to distinguish alleles.

PCR Detection of the Wild-Type *FTSH1* Allele

DNA templates were purified from a pin point of *C. reinhardtii* cells resuspended in 10 μL of water to which was added 10 μL of ethanol and 80 μL of 5% Chelex 100 molecular biology–grade resin (Bio-Rad) and incubated for 8 min at 95°C. One-microliter samples were used in 10-μL reactions performed in a thermocycler (PTC-200; MJ Research) in a PCR buffer containing 1 M betaine, high-fidelity buffer, and polymerase (PCR extender system; 5PRIME). The FtsH1-WTS allele-specific primer 5′-CTGCTGCGCCCCGGCC-3′ was used for the amplification of wild-type *FTSH1* genomic DNA with reverse FtsH1-A3 primer 5′-CGCCCCTTATG-CAGTGCG-3′. At the stringent annealing temperature of 65°C, these primers allowed the detection of the wild-type *FTSH1* allele by specific amplification on genomic DNA of an FtsH1-WTS/FtsH1-A3 product of 277 bp (Supplemental Figure 11).

Chlorophyll Fluorescence Analysis

Fluorescence kinetics were performed with a home-built fluorometer and fluorescence camera (Johnson et al., 2009) by using exponential phase

cultures maintained in aerobic conditions by vigorous agitation in the dark before the experiments. Fluorescence was triggered by continuous actinic light at 590 nm. F_m values were determined in the presence of 10 μM DCMU, an inhibitor of the PSII acceptor side, or by a 250-ms saturating flash delivered between two 150-μs probe pulses, delivered 300 ms apart. Means and SD of two independent experiments for each starvation condition are given.

Protein Isolation and Immunoblot Analysis

For polypeptide analysis, cells were resuspended in 200 mM 1,4-DTT and 200 mM Na_2CO_3 and solubilized in the presence of 2% SDS at 100°C for 50 s. Polypeptides were separated by SDS/urea-PAGE on 12 to 18% SDS-polyacrylamide gels in the presence of 8 M urea (de Vitry et al., 1989), except when indicated differently. Heme peroxidase activity was detected by using 3,3′,5,5′-tetramethylbenzidine (Thomas et al., 1976) or on blots by using chemiluminescence (de Vitry et al., 2004). Proteins were electrotransferred onto Immobilon NC membranes (Westran S membranes; GE Healthcare) in a semidry blotting apparatus at 0.8 mA cm^{-2} for 45 min. Rabbit-specific antibodies against peptides of FtsH1 (DFGRSKSKFQEVPET) or FtsH2 (QVSVDLPDQKGRLEI) were produced and purified by peptide affinity by Eurogentec. For immunodetection by the chemiluminescence method (GE Healthcare), we used antisera against cytochrome b_6, cytochrome *f*, cytochrome b_6f subunit IV, cytochrome b_6f iron-sulfur Rieske protein, PSII extrinsic subunits OEE2 and OEE3, SLT2 (Agrisera AS07 244), and GrpE at a 1:10,000 dilution; ATP synthase CF1 and F1 β-subunit at a 1:100,000 dilution; LhcbM5 (LHCII) at a 1:20,000 dilution; PSII subunits CP43, CP47, and D2 (Agrisera AS06 146) and ClpP1 at a 1:5000 dilution; D1 C terminus (Agrisera AS05 084) at a 1:100,000 dilution; PHOX and D1 DE loop (Agrisera AS10 704) at a 1:8000 dilution; D1 N terminus (Agrisera AS11 1786) at a 1:5000 dilution; FtsH1 of *Arabidopsis thaliana* at a 1:80,000 dilution; FtsH1 and FtsH2 of *C. reinhardtii* at a 1:5000 dilution; Deg5 (Agrisera AS10 703) at a 1:2500 dilution; and CCB2 and CCB4 at a 1:300 dilution.

BN-PAGE and Immunoprecipitations

Membranes were fractionated from sonicated cell lysates (Saint-Marcoux et al., 2009). All steps up to the second dimension analysis were performed at 4°C. Prepared membranes were resuspended in 50 mM Bis-Tris, pH 7.0, 750 mM aminocaproic acid, 0.5 mM EDTA, supplemented with 1× complete EDTA-free protease inhibitor mixture (Roche) at a final chlorophyll concentration of 0.75 mg mL^{-1}. For PSII complex fractionation (Figure 8E), membranes were solubilized by 3% (w/v) freshly prepared *n*-dodecyl-β-D-maltoside for 10 min on ice. Supernatant was collected after centrifugation in a TLA-100 rotor (Beckmann Coulter) at 279,000*g* for 10 min. For FtsH complex fractionation (Figure 3D), membranes were solubilized by 4% (w/v) freshly prepared digitonin for 30 min at 4°C, and supernatant was collected after centrifugation at 16,110*g* for 30 min. For each sample, 10 μL of supernatant (corresponding to 5 μg of chlorophyll) complemented to 0.5% Coomassie Brilliant Blue G 250 was loaded on a precast 3 to 12% NativePAGE Bis-Tris gel (Invitrogen). Electrophoresis was performed with cathode buffer (50 mM Tricine, 15 mM Bis-Tris, pH 7.0, and 0.04% Coomassie Brilliant Blue G 250) and anode buffer (50 mM Bis-Tris, pH 7.0) for 20 min at 50 V and then 2 h at 150 V. For the denaturing second dimension analysis, strips cut from the first dimension gel were incubated at room temperature for 15 min in 2% SDS, 66 mM Na_2CO_3, and 0.67% β-mercaptoethanol and applied on 12% (Figure 8E) or 8% (Figure 3D) SDS-polyacrylamide gels containing 8 M urea for separating PSII subunits and FtsH subunits, respectively. After electrophoresis, protein content was detected by immunoblotting. For immunoprecipitation (Figure 3E), antibodies and preimmune serum were coupled to protein A–Sepharose beads (Schroda et al., 2001). The coupled beads were washed twice in 50 mM Bis-Tris, pH 7.0, 750 mM aminocaproic acid, and 0.5 mM EDTA with 0.25% digitonin and incubated with digitonin-solubilized membranes (prepared as for BN-PAGE) for 1 h at 4°C. Afterward, the coupled beads were washed three times in the previous solution followed by two washes in 10 mM Tris-HCl, pH 7.5. Immunoprecipitated proteins were recovered by boiling the beads in 2% SDS and 12% Suc for 50 s. After centrifugation, the supernatant was complemented to 0.1 M DTT and 0.1 M Na_2CO_3 and analyzed by SDS-PAGE. Protein gel blots of immunoprecipitated samples were detected using horseradish peroxidase–conjugated protein A instead of horseradish peroxidase–conjugated secondary antibodies to decrease the background (Lal et al., 2005).

Photoinhibition

Strains to be compared were diluted from precultures to equal cell densities and cultured for an additional 15 h before photoinhibition (Schroda et al., 1999). Cells at 2 × 10^6 cells mL^{-1} were transferred to 500-mL Erlenmeyer flasks, and these were placed onto equally illuminated spots of a rotary shaker below LEDs. Inhibitors of the translation of chloroplast genes (500 μg mL^{-1} lincomycin and 100 μg mL^{-1} chloramphenicol) were added or not just before photoinhibition. Cells were photoinhibited at 23°C for 1 h at 250 μE m^{-2} s^{-1}. During the light treatment, the temperature of the cultures remained constant. Recovery of photosynthesis was allowed to take place at 6 μE m^{-2} s^{-1}.

Nutrient Starvation

Precultures were grown at 25°C in TAP medium, pH 7.2, at 6 μE m^{-2} s^{-1} or in the dark for nutrient starvations, respectively, in the light or in the dark. For phosphorus starvation, cells of precultures in the exponential phase were washed twice in TAP phosphorus-deprived medium, resuspended at 5 × 10^5 cells mL^{-1}, illuminated at 80 μE m^{-2} s^{-1} or maintained in the dark, washed again, and resuspended to 10^6 cells mL^{-1} after 2 d (Wykoff et al., 1998). For sulfur starvation, cells of precultures in the exponential phase were washed twice in TAP sulfur-deprived medium, resuspended at 5 × 10^5 cells mL^{-1}, and illuminated at 80 μE m^{-2} s^{-1} or maintained in the dark (Wykoff et al., 1998; Zhang et al., 2002). For comparison of sulfur starvation at 80 μE m^{-2} s^{-1} in the presence and absence of acetate, precultures were grown at 25°C in TAP medium at 6 μE m^{-2} s^{-1} followed by 15 h at 80 μE m^{-2} s^{-1} before sulfur starvation. Cells of precultures in the exponential phase were collected, washed twice in TAP sulfur-deprived medium or in minimum sulfur-deprived medium, resuspended at 5 × 10^5 cells mL^{-1}, and maintained at 80 μE m^{-2} s^{-1}.

Accession Numbers

Sequence data from this article can be found in GenBank/Swiss-Prot database under the following accession numbers: Cr-FtsH1, EDP05335.1; Ec-FtsH, AAA23813.1; and Tm-FtsH, Q9WZ49.1.

Supplemental Data

The following materials are available in the online version of this article.

Supplemental Figure 1. Unrooted Phylogenetic Tree of FtsH Proteins.

Supplemental Figure 2. Backcross of *Rccb2-306* mt− with *ccb2* mt+ Yields Only Parental Ditype Tetrads, Showing That the Suppressor Mutation Is Monogenic and Nuclear.

Supplemental Figure 3. Backcross of $Su_{1\text{-}ccb2}$ with *ccb2* Confirms the Suppressor Effect.

Supplemental Figure 4. Map-Based Cloning of the Suppressor.

Supplemental Figure 5. Mutation *ftsh1-1* Is Recessive in Vegetative Diploids.

Supplemental Figure 6. PSII Subunit D1 Did Not Coimmunoprecipitate with the Antibody against the FtsH1 Peptide.

Supplemental Figure 7. Cell Response Is Delayed and Thylakoid Proteases Are Preserved upon Sulfur Starvation When Cell Viability Solely Depends on Photosynthesis.

Supplemental Figure 8. D1/D2 Oligomers Accumulate Only in the *ftsh1-1* Mutant upon Sulfur Starvation in the Dark.

Supplemental Figure 9. *ftsh1-1* Does Not Increase the Accumulation of PSII Integral Subunits Lacking Assembly Partners.

Supplemental Figure 10. D1 Fragments.

Supplemental Figure 11. PCR Test Used to Discriminate between *ftsh1-1* and Wild-Type *FTSH1* Alleles.

Supplemental Data Set 1. FtsH Sequence Alignment of the Sites Retained for the Phylogenetic Analysis.

ACKNOWLEDGMENTS

We thank Dominique Drapier and Alix Boulouis for sharing their expertise in map-based cloning, Yves Choquet for assistance with {Δ*petAD*} mutant construction, Stéphane Lemaire for the pSL18 plasmid, Karim Mouzannar for help in pSL18-*FTSH1* construction, Adrien Quiles, Palak Garg, and Sarah Pousset for assistance with mutant characterization, Olivier Vallon and Nicolas Tourasse for help in FtsH phylogeny, and Arthur Grossman, Kevin Redding, Michael Schroda, Yuichiro Takahashi, and Francesca Zito for PHOX, PsaA, GrpE, LhcbM5, and subunit IV antibodies, respectively. This work was funded by the Agence Nationale de la Recherche (projects ANR-07-BLAN-0114, ANR-12-BSV8-0011-01, and ANR-11-LABX-0011), the European Union (project 245070 FP7-KBBE-2009-3 SUNBIOPATH), and the Unité Mixte de Recherche 7141/Centre National de la Recherche Scientifique/Université Paris 6.

AUTHOR CONTRIBUTIONS

A.M., J.G.-B., and C.d.V. isolated *C. reinhardtii ccb2* revertant strains and did the genetic and molecular analysis. A.M., F.W., F.-A.W., and C.d.V. performed biochemical and physiological analyses of mutant *ftsh1-1* and of strains combining the *ftsh1-1* mutation with assembly mutants of photosynthetic complexes. All authors contributed to designing the study, analyzing the data, and writing the article. C.d.V. coordinated the project.

Received October 29, 2013; revised November 28, 2013; accepted December 18, 2013; published January 21, 2014.

REFERENCES

Abascal, F., Zardoya, R., and Posada, D. (2005). ProtTest: Selection of best-fit models of protein evolution. Bioinformatics **21:** 2104–2105.

Adam, Z., Rudella, A., and van Wijk, K.J. (2006). Recent advances in the study of Clp, FtsH and other proteases located in chloroplasts. Curr. Opin. Plant Biol. **9:** 234–240.

Ahmadian, M.R., Stege, P., Scheffzek, K., and Wittinghofer, A. (1997). Confirmation of the arginine-finger hypothesis for the GAP-stimulated GTP-hydrolysis reaction of Ras. Nat. Struct. Biol. **4:** 686–689.

Allmer, J., Naumann, B., Markert, C., Zhang, M., and Hippler, M. (2006). Mass spectrometric genomic data mining: Novel insights into bioenergetic pathways in *Chlamydomonas reinhardtii*. Proteomics **6:** 6207–6220.

Arlt, H., Steglich, G., Perryman, R., Guiard, B., Neupert, W., and Langer, T. (1998). The formation of respiratory chain complexes in mitochondria is under the proteolytic control of the *m*-AAA protease. EMBO J. **17:** 4837–4847.

Atteia, A., et al. (2009). A proteomic survey of *Chlamydomonas reinhardtii* mitochondria sheds new light on the metabolic plasticity of the organelle and on the nature of the alpha-proteobacterial mitochondrial ancestor. Mol. Biol. Evol. **26:** 1533–1548.

Bailey, S., Thompson, E., Nixon, P.J., Horton, P., Mullineaux, C.W., Robinson, C., and Mann, N.H. (2002). A critical role for the Var2 FtsH homologue of *Arabidopsis thaliana* in the photosystem II repair cycle in vivo. J. Biol. Chem. **277:** 2006–2011.

Baker, N.R. (2008). Chlorophyll fluorescence: A probe of photosynthesis in vivo. Annu. Rev. Plant Biol. **59:** 89–113.

Barker, M., de Vries, R., Nield, J., Komenda, J., and Nixon, P.J. (2006). The deg proteases protect *Synechocystis* sp. PCC 6803 during heat and light stresses but are not essential for removal of damaged D1 protein during the photosystem two repair cycle. J. Biol. Chem. **281:** 30347–30355.

Bieniossek, C., Schalch, T., Bumann, M., Meister, M., Meier, R., and Baumann, U. (2006). The molecular architecture of the metalloprotease FtsH. Proc. Natl. Acad. Sci. USA **103:** 3066–3071.

Boehm, M., Nield, J., Zhang, P., Aro, E.M., Komenda, J., and Nixon, P.J. (2009). Structural and mutational analysis of band 7 proteins in the cyanobacterium *Synechocystis* sp. strain PCC 6803. J. Bacteriol. **191:** 6425–6435.

Boehm, M., Romero, E., Reisinger, V., Yu, J., Komenda, J., Eichacker, L.A., Dekker, J.P., and Nixon, P.J. (2011). Investigating the early stages of photosystem II assembly in *Synechocystis* sp. PCC 6803: Isolation of CP47 and CP43 complexes. J. Biol. Chem. **286:** 14812–14819.

Boehm, M., Yu, J., Krynicka, V., Barker, M., Tichy, M., Komenda, J., Nixon, P.J., and Nield, J. (2012). Subunit organization of a *Synechocystis* hetero-oligomeric thylakoid FtsH complex involved in photosystem II repair. Plant Cell **24:** 3669–3683.

Boynton, J.E., Gillham, N.W., Harris, E.H., Hosler, J.P., Johnson, A.M., Jones, A.R., Randolph-Anderson, B.L., Robertson, D., Klein, T.M., Shark, K.B., and Sanford, J.C. (1988). Chloroplast transformation in *Chlamydomonas* with high velocity microprojectiles. Science **240:** 1534–1538.

Bulté, L., and Wollman, F.A. (1992). Evidence for a selective destabilization of an integral membrane protein, the cytochrome $b_{6/}f$ complex, during gametogenesis in *Chlamydomonas reinhardtii*. Eur. J. Biochem. **204:** 327–336.

Chen, K.M., Piippo, M., Holmström, M., Nurmi, M., Pakula, E., Suorsa, M., and Aro, E.M. (2011). A chloroplast-targeted DnaJ protein AtJ8 is negatively regulated by light and has rapid turnover in darkness. J. Plant Physiol. **168:** 1780–1783.

Choquet, Y., Zito, F., Wostrikoff, K., and Wollman, F.A. (2003). Cytochrome *f* translation in *Chlamydomonas* chloroplast is autoregulated by its carboxyl-terminal domain. Plant Cell **15:** 1443–1454.

Choquet, Y., Stern, D.B., Wostrikoff, K., Kuras, R., Girard-Bascou, J., and Wollman, F.A. (1998). Translation of cytochrome *f* is autoregulated through the 5′ untranslated region of petA mRNA in *Chlamydomonas* chloroplasts. Proc. Natl. Acad. Sci. USA **95:** 4380–4385.

Depège, N., Bellafiore, S., and Rochaix, J.D. (2003). Role of chloroplast protein kinase Stt7 in LHCII phosphorylation and state transition in *Chlamydomonas*. Science **299:** 1572–1575.

de Vitry, C., Desbois, A., Redeker, V., Zito, F., and Wollman, F.A. (2004). Biochemical and spectroscopic characterization of the

covalent binding of heme to cytochrome b_6. Biochemistry **43:** 3956–3968.

de Vitry, C., Olive, J., Drapier, D., Recouvreur, M., and Wollman, F.A. (1989). Posttranslational events leading to the assembly of photosystem II protein complex: A study using photosynthesis mutants from *Chlamydomonas reinhardtii*. J. Cell Biol. **109:** 991–1006.

Drapier, D., Girard-Bascou, J., Stern, D.B., and Wollman, F.A. (2002). A dominant nuclear mutation in *Chlamydomonas* identifies a factor controlling chloroplast mRNA stability by acting on the coding region of the atpA transcript. Plant J. **31:** 687–697.

Eberhard, S., Drapier, D., and Wollman, F.A. (2002). Searching limiting steps in the expression of chloroplast-encoded proteins: relations between gene copy number, transcription, transcript abundance and translation rate in the chloroplast of *Chlamydomonas reinhardtii*. Plant J. **31:** 149–160.

Edelman, M., and Mattoo, A.K. (2008). D1-protein dynamics in photosystem II: The lingering enigma. Photosynth. Res. **98:** 609–620.

Eversole, R.A. (1956). Biochemical mutants of *Chlamydomonas reinhardtii*. Am. J. Bot. **43:** 404–407.

Ferro, M., et al. (2010). AT_CHLORO, a comprehensive chloroplast proteome database with subplastidial localization and curated information on envelope proteins. Mol. Cell. Proteomics **9:** 1063–1084.

Friso, G., Giacomelli, L., Ytterberg, A.J., Peltier, J.B., Rudella, A., Sun, Q., and Wijk, K.J. (2004). In-depth analysis of the thylakoid membrane proteome of *Arabidopsis thaliana* chloroplasts: New proteins, new functions, and a plastid proteome database. Plant Cell **16:** 478–499.

Genty, B., Briantais, J.M., and Baker, N.R. (1989). The relationship between the quantum yield of photosynthetic electron transport and quenching of chlorophyll fluorescence. Biochim. Biophys. Acta **990:** 87–92.

González-Ballester, D., Casero, D., Cokus, S., Pellegrini, M., Merchant, S.S., and Grossman, A.R. (2010). RNA-seq analysis of sulfur-deprived *Chlamydomonas* cells reveals aspects of acclimation critical for cell survival. Plant Cell **22:** 2058–2084.

Guzélin, E., Rep, M., and Grivell, L.A. (1996). Afg3p, a mitochondrial ATP-dependent metalloprotease, is involved in degradation of mitochondrially-encoded Cox1, Cox3, Cob, Su6, Su8 and Su9 subunits of the inner membrane complexes III, IV and V. FEBS Lett. **381:** 42–46.

Hallmann, A. (1999). Enzymes in the extracellular matrix of *Volvox*: An inducible, calcium-dependent phosphatase with a modular composition. J. Biol. Chem. **274:** 1691–1697.

Harris, E.H. (1989). The Chlamydomonas Source Book. (San Diego, CA: Academic Press).

Heinemeyer, J., Eubel, H., Wehmhöner, D., Jänsch, L., and Braun, H.P. (2004). Proteomic approach to characterize the supramolecular organization of photosystems in higher plants. Phytochemistry **65:** 1683–1692.

Herman, C., Prakash, S., Lu, C.Z., Matouschek, A., and Gross, C.A. (2003). Lack of a robust unfoldase activity confers a unique level of substrate specificity to the universal AAA protease FtsH. Mol. Cell **11:** 659–669.

Huesgen, P.F., Schuhmann, H., and Adamska, I. (2009). Deg/HtrA proteases as components of a network for photosystem II quality control in chloroplasts and cyanobacteria. Res. Microbiol. **160:** 726–732.

Ito, K., and Akiyama, Y. (2005). Cellular functions, mechanism of action, and regulation of FtsH protease. Annu. Rev. Microbiol. **59:** 211–231.

Itzhaki, H., Naveh, L., Lindahl, M., Cook, M., and Adam, Z. (1998). Identification and characterization of DegP, a serine protease associated with the luminal side of the thylakoid membrane. J. Biol. Chem. **273:** 7094–7098.

Johnson, X., Vandystadt, G., Bujaldon, S., Wollman, F.A., Dubois, R., Roussel, P., Alric, J., and Béal, D. (2009). A new setup for in vivo fluorescence imaging of photosynthetic activity. Photosynth. Res. **102:** 85–93.

Kapri-Pardes, E., Naveh, L., and Adam, Z. (2007). The thylakoid lumen protease Deg1 is involved in the repair of photosystem II from photoinhibition in *Arabidopsis*. Plant Cell **19:** 1039–1047.

Karata, K., Verma, C.S., Wilkinson, A.J., and Ogura, T. (2001). Probing the mechanism of ATP hydrolysis and substrate translocation in the AAA protease FtsH by modelling and mutagenesis. Mol. Microbiol. **39:** 890–903.

Karata, K., Inagawa, T., Wilkinson, A.J., Tatsuta, T., and Ogura, T. (1999). Dissecting the role of a conserved motif (the second region of homology) in the AAA family of ATPases. Site-directed mutagenesis of the ATP-dependent protease FtsH. J. Biol. Chem. **274:** 26225–26232.

Kashino, Y., Lauber, W.M., Carroll, J.A., Wang, Q., Whitmarsh, J., Satoh, K., and Pakrasi, H.B. (2002). Proteomic analysis of a highly active photosystem II preparation from the cyanobacterium *Synechocystis* sp. PCC 6803 reveals the presence of novel polypeptides. Biochemistry **41:** 8004–8012.

Kato, Y., and Sakamoto, W. (2009). Protein quality control in chloroplasts: A current model of D1 protein degradation in the photosystem II repair cycle. J. Biochem. **146:** 463–469.

Kato, Y., Sun, X., Zhang, L., and Sakamoto, W. (2012). Cooperative D1 degradation in the photosystem II repair mediated by chloroplastic proteases in Arabidopsis. Plant Physiol. **159:** 1428–1439.

Kato, Y., Miura, E., Ido, K., Ifuku, K., and Sakamoto, W. (2009). The variegated mutants lacking chloroplastic FtsHs are defective in D1 degradation and accumulate reactive oxygen species. Plant Physiol. **151:** 1790–1801.

Kley, J., Schmidt, B., Boyanov, B., Stolt-Bergner, P.C., Kirk, R., Ehrmann, M., Knopf, R.R., Naveh, L., Adam, Z., and Clausen, T. (2011). Structural adaptation of the plant protease Deg1 to repair photosystem II during light exposure. Nat. Struct. Mol. Biol. **18:** 728–731.

Komenda, J., Sobotka, R., and Nixon, P.J. (2012). Assembling and maintaining the photosystem II complex in chloroplasts and cyanobacteria. Curr. Opin. Plant Biol. **15:** 245–251.

Komenda, J., Knoppová, J., Krynická, V., Nixon, P.J., and Tichý, M. (2010). Role of FtsH2 in the repair of photosystem II in mutants of the cyanobacterium *Synechocystis* PCC 6803 with impaired assembly or stability of the $CaMn_{(4)}$ cluster. Biochim. Biophys. Acta **1797:** 566–575.

Komenda, J., Barker, M., Kuviková, S., de Vries, R., Mullineaux, C.W., Tichy, M., and Nixon, P.J. (2006). The FtsH protease slr0228 is important for quality control of photosystem II in the thylakoid membrane of *Synechocystis* sp. PCC 6803. J. Biol. Chem. **281:** 1145–1151.

Krzywda, S., Brzozowski, A.M., Verma, C., Karata, K., Ogura, T., and Wilkinson, A.J. (2002). The crystal structure of the AAA domain of the ATP-dependent protease FtsH of *Escherichia coli* at 1.5 A resolution. Structure **10:** 1073–1083.

Kuras, R., and Wollman, F.A. (1994). The assembly of cytochrome b_6f complexes: An approach using genetic transformation of the green alga *Chlamydomonas reinhardtii*. EMBO J. **13:** 1019–1027.

Kuras, R., Saint-Marcoux, D., Wollman, F.A., and de Vitry, C. (2007). A specific *c*-type cytochrome maturation system is required for oxygenic photosynthesis. Proc. Natl. Acad. Sci. USA **104:** 9906–9910.

Kuras, R., de Vitry, C., Choquet, Y., Girard-Bascou, J., Culler, D., Büschlen, S., Merchant, S., and Wollman, F.A. (1997). Molecular genetic identification of a pathway for heme binding to cytochrome b_6. J. Biol. Chem. **272:** 32427–32435.

Kurisu, G., Zhang, H., Smith, J.L., and Cramer, W.A. (2003). Structure of the cytochrome b_6f complex of oxygenic photosynthesis: Tuning the cavity. Science **302:** 1009–1014.

Lal, A., Haynes, S.R., and Gorospe, M. (2005). Clean western blot signals from immunoprecipitated samples. Mol. Cell. Probes **19:** 385–388.

Larkin, M.A., et al. (2007). Clustal W and Clustal X version 2.0. Bioinformatics **23:** 2947–2948.

Le, S.Q., and Gascuel, O. (2008). An improved general amino acid replacement matrix. Mol. Biol. Evol. **25:** 1307–1320.

Lezhneva, L., Kuras, R., Ephritikhine, G., and de Vitry, C. (2008). A novel pathway of cytochrome *c* biogenesis is involved in the assembly of the cytochrome b_6f complex in *Arabidopsis* chloroplasts. J. Biol. Chem. **283:** 24608–24616.

Li, H.H., Quinn, J., Culler, D., Girard-Bascou, J., and Merchant, S. (1996). Molecular genetic analysis of plastocyanin biosynthesis in *Chlamydomonas reinhardtii*. J. Biol. Chem. **271:** 31283–31289.

Lindahl, M., Spetea, C., Hundal, T., Oppenheim, A.B., Adam, Z., and Andersson, B. (2000). The thylakoid FtsH protease plays a role in the light-induced turnover of the photosystem II D1 protein. Plant Cell **12:** 419–431.

Lindahl, M., Tabak, S., Cseke, L., Pichersky, E., Andersson, B., and Adam, Z. (1996). Identification, characterization, and molecular cloning of a homologue of the bacterial FtsH protease in chloroplasts of higher plants. J. Biol. Chem. **271:** 29329–29334.

Majeran, W., Wollman, F.A., and Vallon, O. (2000). Evidence for a role of ClpP in the degradation of the chloroplast cytochrome b_6f complex. Plant Cell **12:** 137–150.

Majeran, W., Olive, J., Drapier, D., Vallon, O., and Wollman, F.A. (2001). The light sensitivity of ATP synthase mutants of *Chlamydomonas reinhardtii*. Plant Physiol. **126:** 421–433.

Malnoë, A., Wollman, F.A., de Vitry, C., and Rappaport, F. (2011). Photosynthetic growth despite a broken Q-cycle. Nat Commun **2:** 301.

Mann, N.H., Novac, N., Mullineaux, C.W., Newman, J., Bailey, S., and Robinson, C. (2000). Involvement of an FtsH homologue in the assembly of functional photosystem I in the cyanobacterium *Synechocystis* sp. PCC 6803. FEBS Lett. **479:** 72–77.

Martin, A., Baker, T.A., and Sauer, R.T. (2005). Rebuilt AAA+ motors reveal operating principles for ATP-fuelled machines. Nature **437:** 1115–1120.

Matagne, R.F. (1978). Fine structure of the arg-7 cistron in *Chlamydomonas reinhardtii*. Complementation between arg-7 mutants defective in argininosuccinate lyase. Mol. Gen. Genet. **160:** 95–99.

Minai, L., Wostrikoff, K., Wollman, F.A., and Choquet, Y. (2006). Chloroplast biogenesis of photosystem II cores involves a series of assembly-controlled steps that regulate translation. Plant Cell **18:** 159–175.

Moldavski, O., Levin-Kravets, O., Ziv, T., Adam, Z., and Prag, G. (2012). The hetero-hexameric nature of a chloroplast AAA+ FtsH protease contributes to its thermodynamic stability. PLoS ONE **7:** e36008.

Moseley, J.L., Chang, C.W., and Grossman, A.R. (2006). Genome-based approaches to understanding phosphorus deprivation responses and PSR1 control in *Chlamydomonas reinhardtii*. Eukaryot. Cell **5:** 26–44.

Narberhaus, F., Obrist, M., Führer, F., and Langklotz, S. (2009). Degradation of cytoplasmic substrates by FtsH, a membrane-anchored protease with many talents. Res. Microbiol. **160:** 652–659.

Neuwald, A.F., Aravind, L., Spouge, J.L., and Koonin, E.V. (1999). AAA+: A class of chaperone-like ATPases associated with the assembly, operation, and disassembly of protein complexes. Genome Res. **9:** 27–43.

Nixon, P.J., Michoux, F., Yu, J., Boehm, M., and Komenda, J. (2010). Recent advances in understanding the assembly and repair of photosystem II. Ann. Bot. (Lond.) **106:** 1–16.

Ogura, T., Whiteheart, S.W., and Wilkinson, A.J. (2004). Conserved arginine residues implicated in ATP hydrolysis, nucleotide-sensing, and inter-subunit interactions in AAA and AAA+ ATPases. J. Struct. Biol. **146:** 106–112.

Ostersetzer, O., and Adam, Z. (1997). Light-stimulated degradation of an unassembled Rieske FeS protein by a thylakoid-bound protease: The possible role of the FtsH protease. Plant Cell **9:** 957–965.

Piechota, J., Kolodziejczak, M., Juszczak, I., Sakamoto, W., and Janska, H. (2010). Identification and characterization of high molecular weight complexes formed by matrix AAA proteases and prohibitins in mitochondria of *Arabidopsis thaliana*. J. Biol. Chem. **285:** 12512–12521.

Pootakham, W., Gonzalez-Ballester, D., and Grossman, A.R. (2010). Identification and regulation of plasma membrane sulfate transporters in *Chlamydomonas*. Plant Physiol. **153:** 1653–1668.

Rodrigues, R.A., Silva-Filho, M.C., and Cline, K. (2011). FtsH2 and FtsH5: Two homologous subunits use different integration mechanisms leading to the same thylakoid multimeric complex. Plant J. **65:** 600–609.

Rodriguez, F., Arsène-Ploetze, F., Rist, W., Rüdiger, S., Schneider-Mergener, J., Mayer, M.P., and Bukau, B. (2008). Molecular basis for regulation of the heat shock transcription factor sigma32 by the DnaK and DnaJ chaperones. Mol. Cell **32:** 347–358.

Rymarquis, L.A., Handley, J.M., Thomas, M., and Stern, D.B. (2005). Beyond complementation. Map-based cloning in *Chlamydomonas reinhardtii*. Plant Physiol. **137:** 557–566.

Saikawa, N., Akiyama, Y., and Ito, K. (2004). FtsH exists as an exceptionally large complex containing HflKC in the plasma membrane of *Escherichia coli*. J. Struct. Biol. **146:** 123–129.

Saint-Marcoux, D., Wollman, F.A., and de Vitry, C. (2009). Biogenesis of cytochrome b_6 in photosynthetic membranes. J. Cell Biol. **185:** 1195–1207.

Sakamoto, W. (2006). Protein degradation machineries in plastids. Annu. Rev. Plant Biol. **57:** 599–621.

Sakamoto, W., Zaltsman, A., Adam, Z., and Takahashi, Y. (2003). Coordinated regulation and complex formation of YELLOW VARIEGATED1 and YELLOW VARIEGATED2, chloroplastic FtsH metalloproteases involved in the repair cycle of photosystem II in *Arabidopsis* thylakoid membranes. Plant Cell **15:** 2843–2855.

Schroda, M., and Vallon, O. (2009). Chaperones and proteases. In The *Chlamydomonas* Sourcebook: Organellar and Metabolic Processes, D. Stern, ed (Ithaca, NY: Academic Press), pp. 671–729.

Schroda, M., Vallon, O., Wollman, F.A., and Beck, C.F. (1999). A chloroplast-targeted heat shock protein 70 (HSP70) contributes to the photoprotection and repair of photosystem II during and after photoinhibition. Plant Cell **11:** 1165–1178.

Schroda, M., Vallon, O., Whitelegge, J.P., Beck, C.F., and Wollman, F.A. (2001). The chloroplastic GrpE homolog of *Chlamydomonas*: Two isoforms generated by differential splicing. Plant Cell **13:** 2823–2839.

Shimogawara, K., Fujiwara, S., Grossman, A., and Usuda, H. (1998). High-efficiency transformation of *Chlamydomonas reinhardtii* by electroporation. Genetics **148:** 1821–1828.

Silva, P., Thompson, E., Bailey, S., Kruse, O., Mullineaux, C.W., Robinson, C., Mann, N.H., and Nixon, P.J. (2003). FtsH is involved in the early stages of repair of photosystem II in *Synechocystis* sp PCC 6803. Plant Cell **15:** 2152–2164.

Sinvany-Villalobo, G., Davydov, O., Ben-Ari, G., Zaltsman, A., Raskind, A., and Adam, Z. (2004). Expression in multigene families. Analysis of chloroplast and mitochondrial proteases. Plant Physiol. **135:** 1336–1345.

Sokolenko, A., Pojidaeva, E., Zinchenko, V., Panichkin, V., Glaser, V.M., Herrmann, R.G., and Shestakov, S.V. (2002). The gene complement for proteolysis in the cyanobacterium Synechocystis

sp. PCC 6803 and *Arabidopsis thaliana* chloroplasts. Curr. Genet. **41:** 291–310.

Stamatakis, A. (2006). RAxML-VI-HPC: Maximum likelihood-based phylogenetic analyses with thousands of taxa and mixed models. Bioinformatics **22:** 2688–2690.

Steglich, G., Neupert, W., and Langer, T. (1999). Prohibitins regulate membrane protein degradation by the m-AAA protease in mitochondria. Mol. Cell. Biol. **19:** 3435–3442.

Stroebel, D., Choquet, Y., Popot, J.L., and Picot, D. (2003). An atypical haem in the cytochrome b_6f complex. Nature **426:** 413–418.

Sun, Q., Zybailov, B., Majeran, W., Friso, G., Olinares, P.D., and van Wijk, K.J. (2009). PPDB, the Plant Proteomics Database at Cornell. Nucleic Acids Res. **37:** D969–D974.

Sun, X., Peng, L., Guo, J., Chi, W., Ma, J., Lu, C., and Zhang, L. (2007). Formation of DEG5 and DEG8 complexes and their involvement in the degradation of photodamaged photosystem II reaction center D1 protein in *Arabidopsis*. Plant Cell **19:** 1347–1361.

Sun, X., Fu, T., Chen, N., Guo, J., Ma, J., Zou, M., Lu, C., and Zhang, L. (2010). The stromal chloroplast Deg7 protease participates in the repair of photosystem II after photoinhibition in Arabidopsis. Plant Physiol. **152:** 1263–1273.

Suno, R., Niwa, H., Tsuchiya, D., Zhang, X., Yoshida, M., and Morikawa, K. (2006). Structure of the whole cytosolic region of ATP-dependent protease FtsH. Mol. Cell **22:** 575–585.

Suzuki, C.K., Rep, M., van Dijl, J.M., Suda, K., Grivell, L.A., and Schatz, G. (1997). ATP-dependent proteases that also chaperone protein biogenesis. Trends Biochem. Sci. **22:** 118–123.

Thomas, P.E., Ryan, D., and Levin, W. (1976). An improved staining procedure for the detection of the peroxidase activity of cytochrome P-450 on sodium dodecyl sulfate polyacrylamide gels. Anal. Biochem. **75:** 168–176.

Van Dyck, L., and Langer, T. (1999). ATP-dependent proteases controlling mitochondrial function in the yeast *Saccharomyces cerevisiae*. Cell. Mol. Life Sci. **56:** 825–842.

Vermaas, W.F. (1998). Gene modifications and mutation mapping to study the function of photosystem II. Methods Enzymol. **297:** 293–310.

Wagner, R., Aigner, H., and Funk, C. (2012). FtsH proteases located in the plant chloroplast. Physiol. Plant. **145:** 203–214.

Wei, L., Derrien, B., Gautier, A., Houille-Vernes, L., Boulouis, A., Saint-Marcoux, D., Malnoë, A., Rappaport, F., de Vitry, C., Vallon, O., Choquet, Y., and Wollman, F.-A. (2014). Nitric oxide–triggered remodeling of chloroplast bioenergetics and thylakoid proteins upon nitrogen starvation in *Chlamydomonas reinhardtii*. Plant Cell **26:** 353–372.

Wollman, F.A., Minai, L., and Nechushtai, R. (1999). The biogenesis and assembly of photosynthetic proteins in thylakoid membranes1. Biochim. Biophys. Acta **1411:** 21–85.

Wykoff, D.D., Davies, J.P., Melis, A., and Grossman, A.R. (1998). The regulation of photosynthetic electron transport during nutrient deprivation in *Chlamydomonas reinhardtii*. Plant Physiol. **117:** 129–139.

Yamamoto, Y., Aminaka, R., Yoshioka, M., Khatoon, M., Komayama, K., Takenaka, D., Yamashita, A., Nijo, N., Inagawa, K., Morita, N., Sasaki, T., and Yamamoto, Y. (2008). Quality control of photosystem II: Impact of light and heat stresses. Photosynth. Res. **98:** 589–608.

Yoshioka, M., and Yamamoto, Y. (2011). Quality control of photosystem II: Where and how does the degradation of the D1 protein by FtsH proteases start under light stress? Facts and hypotheses. J. Photochem. Photobiol. B **104:** 229–235.

Yoshioka, M., Nakayama, Y., Yoshida, M., Ohashi, K., Morita, N., Kobayashi, H., and Yamamoto, Y. (2010). Quality control of photosystem II: FtsH hexamers are localized near photosystem II at grana for the swift repair of damage. J. Biol. Chem. **285:** 41972–41981.

Yu, F., Park, S., and Rodermel, S.R. (2004). The *Arabidopsis* FtsH metalloprotease gene family: Interchangeability of subunits in chloroplast oligomeric complexes. Plant J. **37:** 864–876.

Zaltsman, A., Ori, N., and Adam, Z. (2005). Two types of FtsH protease subunits are required for chloroplast biogenesis and photosystem II repair in *Arabidopsis*. Plant Cell **17:** 2782–2790.

Zhang, L., Happe, T., and Melis, A. (2002). Biochemical and morphological characterization of sulfur-deprived and H_2-producing *Chlamydomonas reinhardtii* (green alga). Planta **214:** 552–561.

Zhang, Z., Shrager, J., Jain, M., Chang, C.W., Vallon, O., and Grossman, A.R. (2004). Insights into the survival of *Chlamydomonas reinhardtii* during sulfur starvation based on microarray analysis of gene expression. Eukaryot. Cell **3:** 1331–1348.

Zienkiewicz, M., Ferenc, A., Wasilewska, W., and Romanowska, E. (2012). High light stimulates Deg1-dependent cleavage of the minor LHCII antenna proteins CP26 and CP29 and the PsbS protein in *Arabidopsis thaliana*. Planta **235:** 279–288.

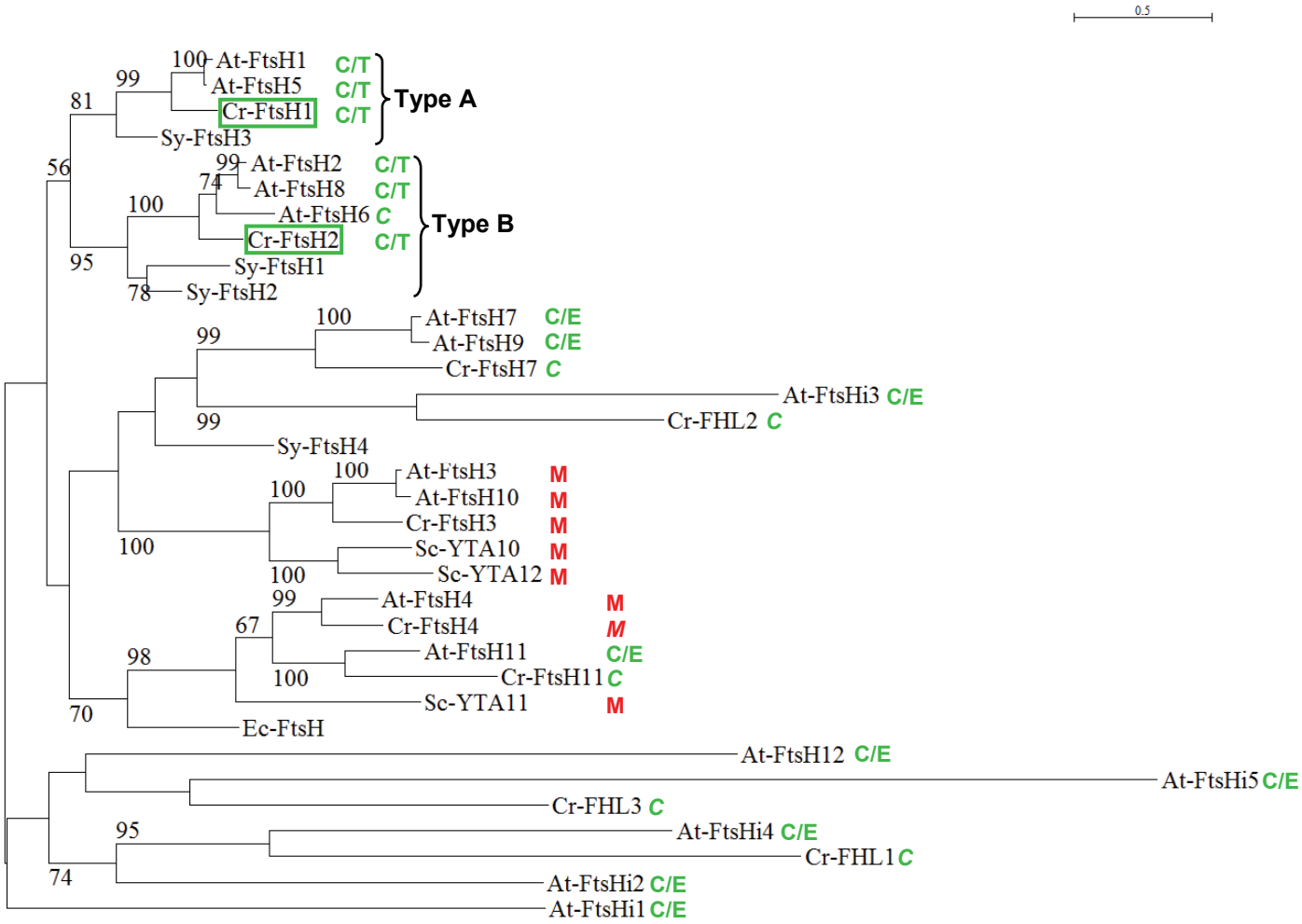

Supplemental Figure 1. Unrooted Phylogenetic Tree of FtsH Proteins.

Nuclear encoded FtsH sequences of *Arabidopsis thaliana* (At) and *Chlamydomonas reinhardtii* (Cr) were obtained from Phytosome v9.1 (http://www.phytozome.net/), FtsH sequences of *Synechocystis* sp. PCC 6803 (Sy) from cyanobase (http://genome.microbedb.jp/cyanobase/), and FtsH sequences of *Escherichia coli* (Ec) and *Saccharomyces cerevisiae* (Sc) from NCBI (http://www.ncbi.nlm.nih.gov/protein): At-FtsH1-12, At-FtsHi1 (AT4G23940), At-FtsHi2 (AT3G16290), At-FtsHi3 (AT3G02450), At-FtsHi4 (AT5G64580), At-FtsHi5 (AT3G04340), Cr-FtsH1 (Cre12.g485800), Cr-FtsH2 (Cre17.g720050), Cr-FtsH3 (Cre01.g019850), Cr-FtsH4 (Cre13.g568400), Cr-FtsH7 (g1437), Cr-FtsH11 (g15070), Cr-FHL1 (Cre03.g201100), Cr-FHL2 (Cre09.g393950), Cr-FHL3 (Cre07.g352350), Sy-FtsH1 (slr1390), Sy-FtsH2 (slr0228), Sy-FtsH3 (slr1604), Sy-FtsH4 (sll1463), Ec-FtsH and Sc-YTA10-12. FtsH-like proteins lacking the Zn-binding motif are annotated At-FtsHi and Cr-FHL. 639 sites were retained for the phylogenetic analysis (see Methods and Supplemental Data Set 1). Cr-FHL2 and At-FtsHi3 sequences are shorter of about 200 amino-acids at their C-terminus and miss part of the protease domain. Bootstrap values above 50% are indicated. The scale bar represents the average number of amino-acids changes per site. The major subcellular localizations of eukaryotic FtsHs, in chloroplasts (in green) or mitochondria (in red), are indicated as determined by proteomic and green fluorescent protein studies (in bold) or as predicted (in italics): chloroplast (C), thylakoid membrane (T) with subunit type (A or B), envelope (E), and mitochondrion (M).

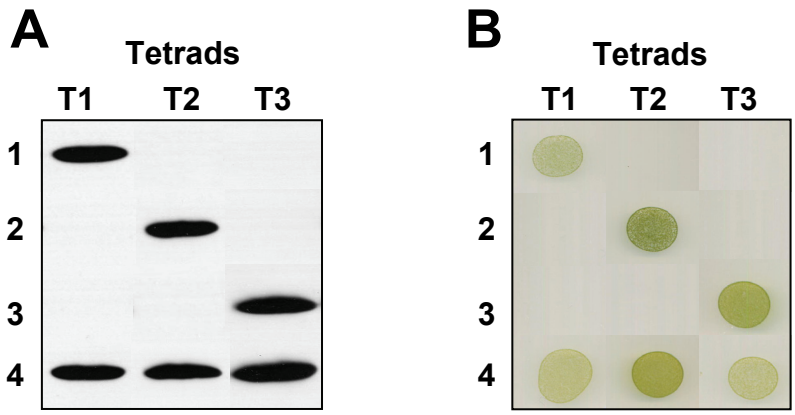

Supplemental Figure 2. Back-Cross of *Rccb2-306* mt- with *ccb2* mt+ Yields only Parental Ditype Tetrads Showing that the Suppressor Mutation is Monogenic and Nuclear.

(A) Mendelian segregation of b_6f complex accumulation as monitored by immunodetection of subunit IV shown here for three tetrads (T).
(B) Phototrophic growth on minimum media segregates as b_6f accumulation.

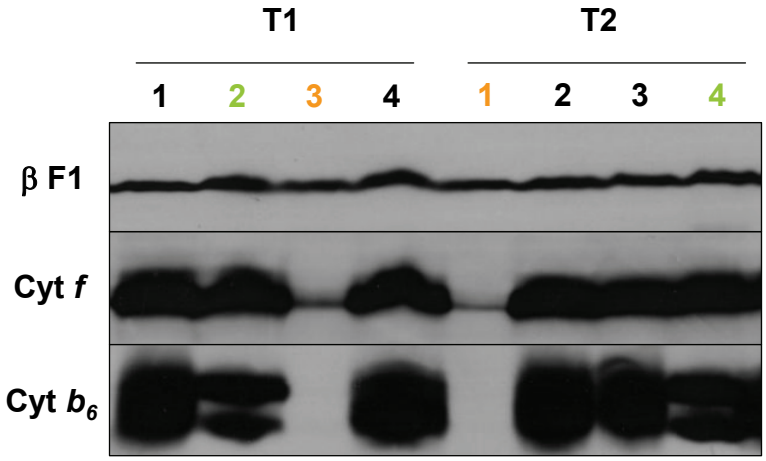

Supplemental Figure 3. Back-Cross of *Su*$_{1\text{-}ccb2}$ with *ccb2* confirms the suppressor effect.

Total cell proteins of two tetratype tetrads (T) grown on acetate medium at 6 µE m^{-2} s^{-1} were separated by SDS/urea-PAGE and the segregation of cytochrome *b*$_6$*f* complex accumulation is monitored by immunodetection of cytochrome *f* (Cyt *f*) and cytochrome *b*$_6$ (Cyt *b*$_6$) using ATP synthase β subunit (β F1) as loading control. *Su*$_{1\text{-}ccb2}$ *ccb2* progeny (in green) has a wild-type accumulation of *b*$_6$*f* subunits with cytochrome *b*$_6$ lacking covalent heme *c*$_i$ while *ccb2* progeny (in orange) accumulates very low amounts of *b*$_6$*f* subunits. When cytochrome *b*$_6$ contains covalent heme *c*$_i$, it shows up as a diffuse band; when it lacks covalent heme *c*$_i$, it shows up as a doublet band under these SDS/urea-PAGE conditions. This correlation is demonstrated in Figure 1B by showing immunoblot of cytochrome *b*$_6$ together with the heme peroxidasic activity assay using tetramethylbenzamidine.

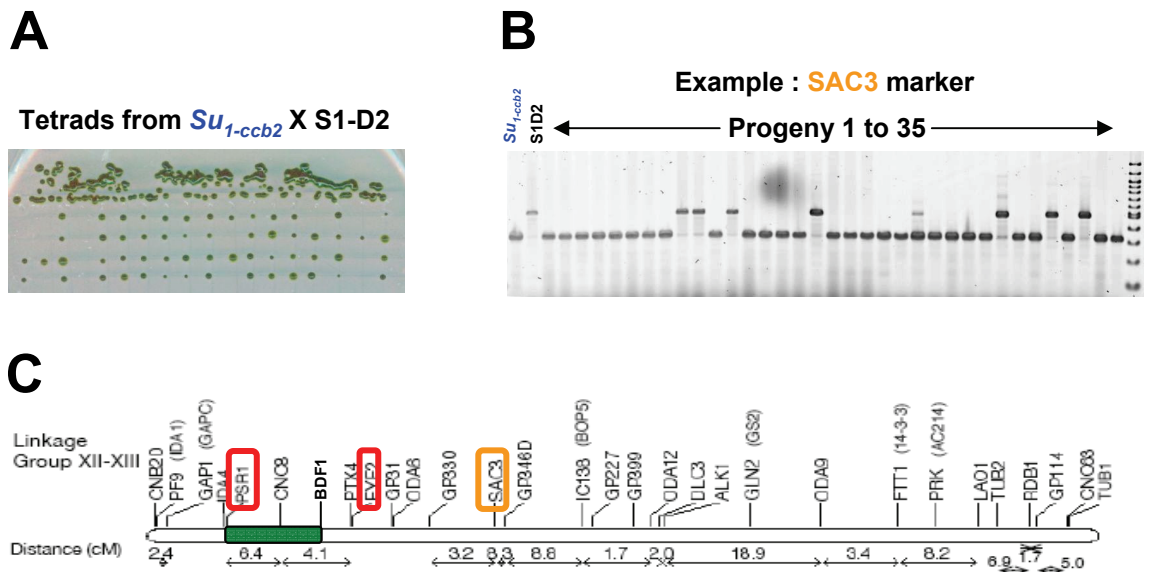

Supplemental Figure 4. Map-Based Cloning of the Suppressor.

(A) Tetrads from the cross of *Chlamydomonas reinhardtii* $Su_{1\text{-}ccb2}$ with the interfertile *Chlamydomonas grossii* specie S1-D2.
(B) Linkage analysis of $Su_{1\text{-}ccb2}$ mutation to SAC3 marker by PCR; the primers used in a single PCR reaction generate products that differ in size for the *reinhardtii* or *grossii* allele.
(C) *Chlamydomonas reinhardtii* linkage group XII-XIII depicted as a long horizontal rod with known genetic distances between markers (cM) shown by two-headed arrows as published in (Merchant, S. et al. (2007) Science 318: 245-250). The suppressor mutation $Su_{1\text{-}ccb2}$ was localized in the vicinity of the PSR1 and BDF1 markers.

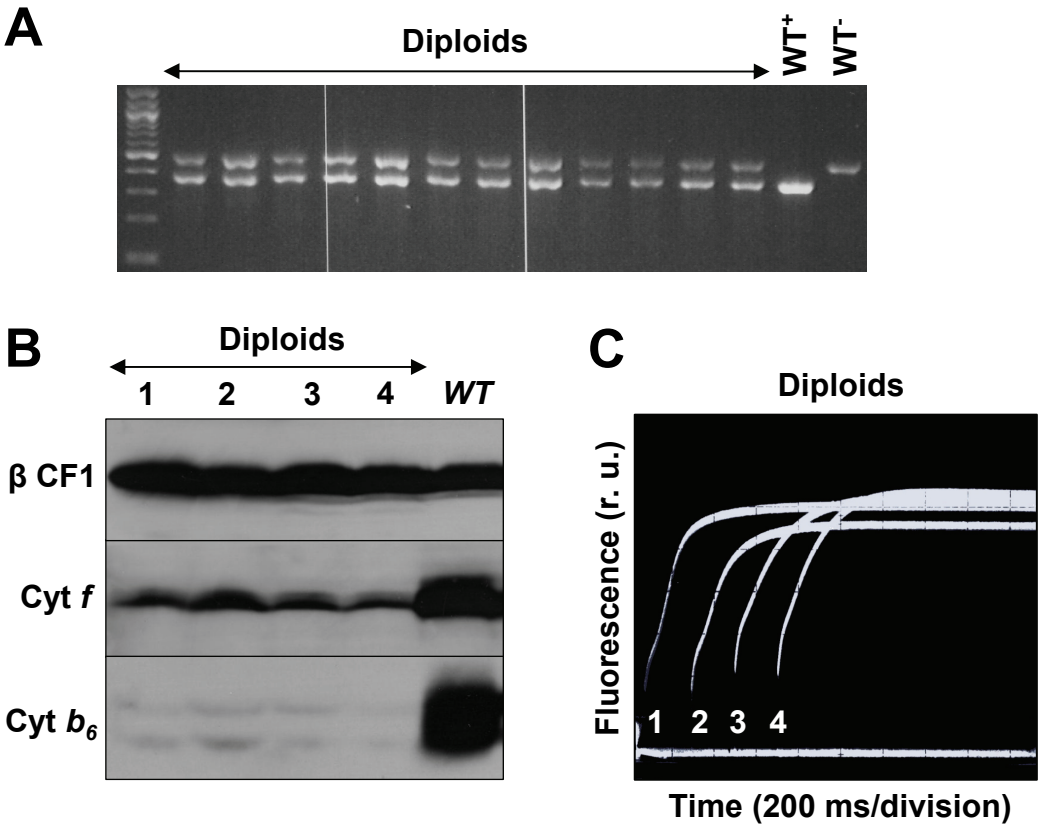

Supplemental Figure 5. Mutation *ftsh1-1* is Recessive in Vegetative Diploids.

(A) PCR mating type test confirms the presence of both mating types in vegetative diploids growing in absence of arginine from cross of *ftsh1-1 ccb2 arg7* with *FTSH1 ccb2 arg2*.
(B) Total cell proteins of vegetative diploids from cross *ftsh1-1 ccb2 arg7* X *FTSH1 ccb2 arg2* separated by SDS/urea-PAGE and analyzed by immunodetection with antibodies against cytochrome b_6f subunits show a low b_6f complex accumulation as in the *ccb2* mutant (Figure 2A).
(C) Vegetative diploids from *ftsh1-1 ccb2 arg7* X *FTSH1 ccb2 arg2* show a b_6f deficiency in fluorescence induction kinetics as the *ccb2* mutant (Figure 2B).

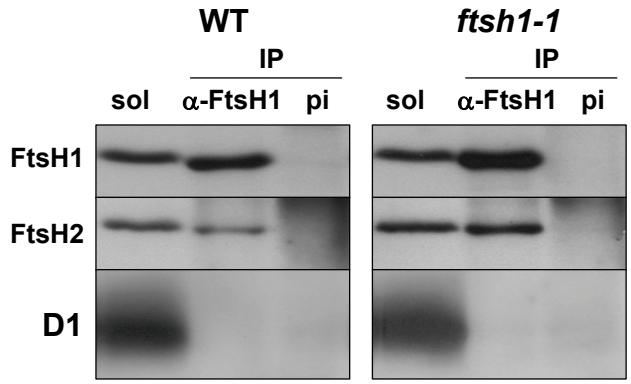

Supplemental Figure 6. PSII subunit D1 did not co-immunoprecipitate with the antibody against FtsH1 peptide.

Digitonin-solubilized membranes from wild-type and *ftsh1-1* strains were incubated with protein A-sepharose beads coupled to antibodies against a peptide of FtsH1 (α-FtsH1) or preimmune serum (pi). Aliquots of digitonin-solubilized membranes (sol) and immunoprecipitates (IP) were separated by SDS-PAGE on a 8% polyacrylamide gel in the presence of 8 M urea and analyzed by immunodetection with antibodies against FtsH1, FtsH2 and D1.

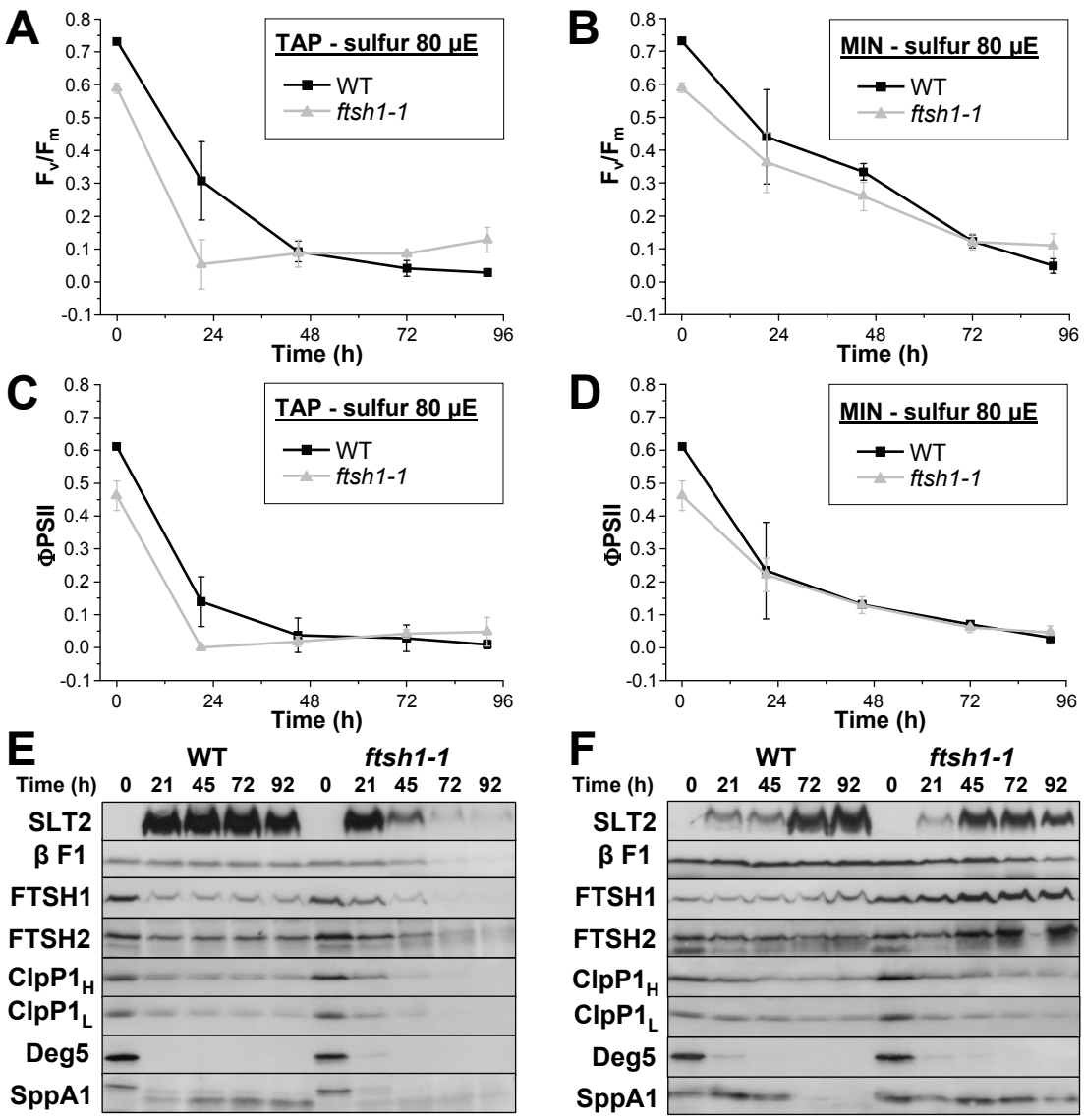

Supplemental Figure 7. Cell Response is Delayed and Thylakoid Proteases are Preserved upon Sulfur Starvation when Cell Viability Solely Depends on Photosynthesis.

(A) Time course of sulfur starvation in the presence of acetate under 80 µE m^{-2} s^{-1} in wild-type and *ftsh1-1* strains as monitored by PSII activity (F_v/F_m).
(B) Time course of sulfur starvation in the absence of acetate under 80 µE m^{-2} s^{-1} as monitored by PSII activity detection.
(C) Time course of sulfur starvation in the presence of acetate under 80 µE m^{-2} s^{-1} as monitored by downstream electron transfer (ΦPSII).
(D) Time course of sulfur starvation in the absence of acetate under 80 µE m^{-2} s^{-1} as monitored by downstream electron transfer detection.
(E) Time course upon sulfur starvation in the presence of acetate under 80 µE m^{-2} s^{-1} as monitored by immunodetection of chloroplast proteases of the thylakoid (FtsH1, FtsH2, SppA1), stroma (unprocessed $ClpP1_H$ and processed $ClpP1_L$) and lumen (Deg5), a marker of the cell response to sulfur deprivation (SLT2) and loading control ATP synthase β subunit (β F1). Total cell proteins were separated by SDS/urea-PAGE.
(F) Time course upon sulfur starvation in the absence of acetate under 80 µE m^{-2} s^{-1} as monitored by immunodetection.
Means and standard deviations of two independent experiments for each starvation condition are given.

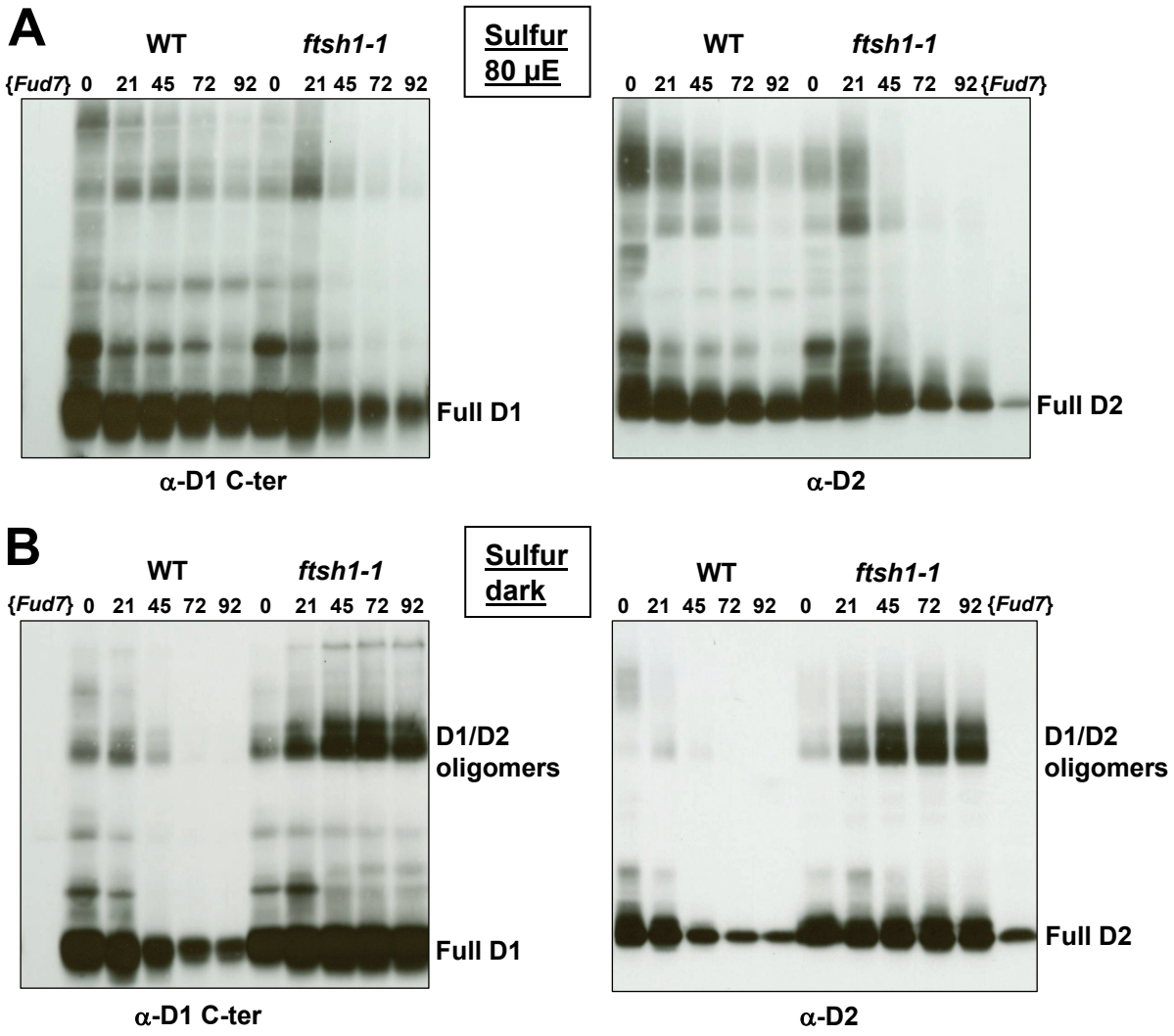

Supplemental Figure 8. D1/D2 Oligomers Accumulate Only in *ftsh1-1* Mutant upon Sulfur Starvation in the Dark.

(A) Time course of sulfur starvation under 80 µE m^{-2} s^{-1} in wild-type and *ftsh1-1* strains as monitored by immunodetection of PSII subunits D1 and D2 and their oligomers. The {*Fud7*} mutant containing a deletion in the chloroplast *psbA* gene which encodes D1 protein is used as a negative D1 control. Total cell proteins were separated on a denaturing 7.5-15% polyacrylamide gel in the presence of 8 M urea.
(B) Time course of sulfur starvation in the dark.

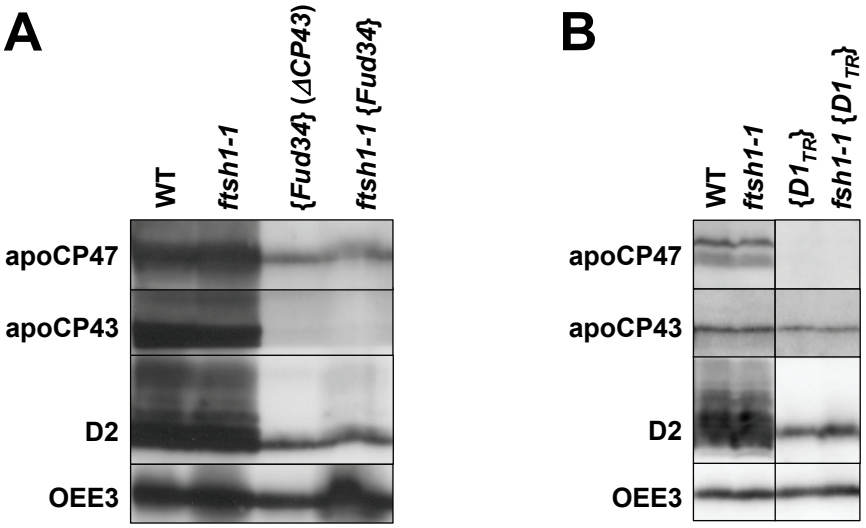

Supplemental Figure 9. *ftsh1-1* Does not Increase Accumulation of PSII Integral Subunits Lacking Assembly Partners.

(A) No overaccumulation of D2 or apoCP47 when apoCP43 is missing {*Fud34*} in *ftsh1-1* context. Total cell proteins were separated on a 12-18% polyacrylamide gel and analyzed by immunodetection.
(B) Not more of D2, CP47 or CP43 when D1 is truncated {*D1TR*} in *ftsh1-1* context; total cell proteins were separated on a 16 % polyacrylamide gel and analyzed by immunodetection.

A

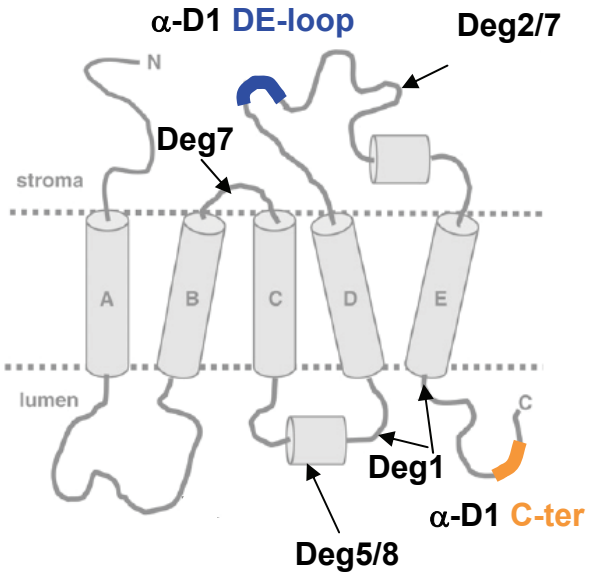

B

D1 fragments probed with α-D1 DE-loop

~ **23 kDa**	Deg2/7 cleavage in DE loop

D1 fragments probed with α-D1 C-ter

~**16 kDa**	Deg7 cleavage in BC loop Deg5/8 cleavage in CD loop Deg1 cleavage in CD loop
~ **6 kDa**	Deg2/7 cleavage in DE loop Deg1 cleavage after TMH E

Supplemental Figure 10. D1 Fragments.

(A) D1 model (adapted from (Kapri-Pardes et al., 2007)) with the localization of Deg cleavage sites from *Arabidopsis* studies (Kapri-Pardes et al., 2007; Kato and Sakamoto, 2009; Kato et al., 2012; Sun et al., 2010) and localization of the D1 DE-loop and C-ter peptides.
(B) Obtained D1 fragments in *Chlamydomonas* detected with D1 DE-loop and C-ter antibodies and corresponding fragments predicted by the *Arabidopsis* model.

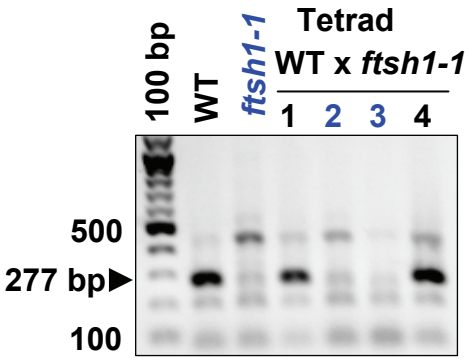

Supplemental Figure 11. PCR Test Used to Discriminate Between *ftsh1-1* and Wild-Type *FTSH1* alleles.

The wild-type genomic DNA *FTSH1* allele is specifically amplified with FtsH1-WTS and FtsH1-A3 primers as a 277 bp product. PCR products of wild-type, *ftsh1-1* and a tetrad progeny from a wild-type and *ftsh1-1* cross were separated on a 1% agarose gel together with a 100 bp DNA ladder.